The adaptive immune responses to SARS-CoV-2 as a recall response susceptible to immune imprinting

Daniel Alvarez-Sierra[1#], Mónica Martínez-Gallo[1,2,3], Adrián Sánchez-Montalvá[4,5,6], Marco Fernández- Sanmartín[7‡], Roger Colobran[1,2,3], Juan Espinosa-Pereiro[4,5,6], Elísabet Poyatos-Canton[8™], Coral Zurera-Egea[10], Alex Sánchez-Pla[11], Concepción Violan[12], Rafael Parra[13], Hammad Alzayat[7‡], Ana Vivancos[14], Francisco Morandeira-Rego[8], Blanca Urban-Vargas[8√], Eva Martínez-Cáceres[3,9,10], Manuel Hernández-González[1,2,3], Aina Teniente-Serra[3,9,10], Jordi Bas- Minguet[8], Peter D. Katsikis[15], Ricardo Pujol-Borrell[2,3,14,*].

1. Translational Immunology Research Group, Vall d'Hebron Research Institute (VHIR), Campus Vall Hebron, Barcelona, Spain.

2. Immunology Department, Hospital Universitari Vall d'Hebron, Campus Vall d'Hebron, Barcelona, Spain.

3. Department of Cell Biology, Physiology, and Immunology, Universitat Autònoma Barcelona, Campus Vall Hebron and Campus Bellaterra, Barcelona, Spain

4. Infectious Disease Department, Hospital Universitari Vall d'Hebron, Campus Vall dHebro, Barcelona, Spain.

5. International Health Program - Institut Català de la Salut, Vall d'Hebron Research Institute (VHIR), Campus Vall Hebron, Barcelona, Spain.

6. Centro de Investigación Biomédica en Red de Enfermedades Infecciosas (CIBERINFEC), Instituto de Salud Carlos III. Campus Vall Hebron, Barcelona.

7. Flow Cytometry Laboratory. Germans Trias Pujol Research Institute (IGTP), Badalona, Barcelona, Spain.

8. Immunology Division, Bellvitge University Hospital, Hospitalet de Llobregat, Barcelona, Spain

9. Immunology Division, Germans Trias Pujol University Hospital, Badalona, Barcelona, Spain

10. Immunology and Inflammation, Research Group, Germans Trias Pujol Research Institute (IGTP), Badalona, Barcelona, Spain

11. Bioinformatics and Statistics Group, University of Barcelona, Barcelona, Spain.

12. Unitat de Suport a la Recerca Metropolitana Nord, Institut Universitari d'Investigació en Atenció Primària Jordi Gol (IDIAP Jordi Gol), Mataró, Barcelona, Spain.

13. Banc de Sang i Teixits, Hospital Universitari Vall Hebron, Barcelona, Spain.

14. Cancer Genomics Group, Vall Hebron Institut Oncology (VHIO), Campus Vall d'Hebron, Barcelona, Spain.

15. Dept. of Immunology; Erasmus University Medical Center, Rotterdam, The Netherlands.

***Correspondence:**
Ricardo Pujol-Borrell MD, PhD
Vall d'Hebron Institute of Oncology
Natzaret 115-117, 08035, Barcelona, Spain
Tel. +34 932543450 Ext. 8682
Email: rpujol@vhio.net

Present addresses
[#]Group of Immunopathology
Marques de Valdecilla Research Institute (IDIVAL)
Cardenal Herrera Orio s/n
39011 Santander, Spain

[‡]Clinical Flow Cytometry Platform
Biomedical Dagnostic Center
Hospital Clinic
University of Barcelona
Villarroel 170
08036 Barcelona

[™]Immunology Laboratory
Pg. de Sant Joan de Déu, 2,
08950 Esplugues de Llobregat,
Barcelona

[√]Immunology Dpt
Immunology Department,
Hospital Universitari Vall d'Hebron,
Campus Vall d'Hebron,
08035 Barcelona, Spain.

All authors declare that they have no conflicts of interest.

ABSTRACT

One possible determinant of COVID-19 severity is immune imprinting (IP) by Common Cold Coronavirus (CCCV). As IP occurs only in recall immune responses, we investigated the immune response to SARS-CoV-2 in a cohort of unvaccinated individual to determine whether their immune response aligned with the primary or recall immune response patterns.

Analysis of the Ig isotype response trajectories to the Mpro, NP, and S structural proteins and the S RBD in this group of 191 patients and 44 controls revealed a pattern of recall response in 94.2 % of cases. The levels of antibodies correlated positively with the severity of the condition rather than a milder course. High-resolution flow cytometry of fresh PBMNCs showed trajectories of plasmablasts, B cell subsets, and cTfh, suggesting a recall response. The transcriptomic profile demonstrated that this group was directly comparable to other contemporary cohorts. Overall, these findings support the idea that the response to SARS-CoV-2 is, in most cases, a recall response, likely due to B and T memory cells to CCCV, and therefore susceptible to immune imprinting and antibody-dependent enhancement.

INTRODUCTION

The COVID-19 pandemic has resulted in over 775 million cases of clinical infections and 7 million deaths worldwide as of August 2024. (https://data.who.int/dashboards/covid19). Even after unprecedented extensive research, some critical questions still demand answers. One of the most debated issues is what causes tissue damage in severe COVID-19. Such damage could be due to virus cytopathic effects, immune-mediated pathology, or a combination of both (1). Understanding the pathogenesis of acute COVID-19 will also help to advance research on long COVID, where uncertainty remains on whether symptoms are due to persistent infection, a dysregulated immune response, or other still-to-be-defined mechanisms (2).

The clinical severity of COVID-19 varies greatly, ranging from no symptoms to death. A proportion of this variability can be attributed to some well-established host risk factors identified in the early stages of the pandemic, in order of importance: age, sex, and comorbidities such as hypertension, diabetes, obesity, chronic lung disease, chronic kidney disease, and immunosuppression (3). Mutations have been identified by the candidate gene approach targeting the type I IFN pathway, accounting for approximately 3% of severe cases (4, 5). Autoantibodies to type-I IFNs explain a proportion of severe cases (6). Dysfunction of the Type I IFN pathway by a gene defect of autoantibodies may explain up to 20% of severe cases (5). A recent COVID-19 Host Genetics Initiative (HGI) meta-analysis identified 21 loci associated with susceptibility and 40 loci associated with COVID-19 hospitalization. These loci accounted for 1.2% and 5.8% of phenotypic variation, respectively (7). The total heritability of severity has been estimated to be 41% (9), but, at present, a significant proportion of COVID-19 severity attributable to the host remains unexplained, as detected in the multivariate analyses part of our previous reports (8).

Some early reports indicated that in COVID-19, the response of IgA and IgG antibodies to SARS-CoV-2 proteins preceded or was contemporary to IgM (9, 10). This is surprising because, in a typical immune response, IgM always precedes IgG and IgA (11, 12). Two explanations have been advanced for this observation: 1) a dysregulation of B cells with a failure to develop germinal centers, thus leading to a prolonged extrafollicular but switched immune response (13), and 2) interference of the immune response to SARS-CoV-2 proteins by pre-existing cross-reactive immunity, a mechanism known as Immune Imprinting (IP) (14). First described as original antigenic sin by T Francis in 1960 (15), IP is also known as antigenic imprinting and primary addiction (16), though these terms are not precisely synonymous. Original antigenic sin has been linked to antibody-dependent enhancement (ADE), which was first described in dengue (17) but may occur after other viral infections (16) and occasionally

vaccination (18). In ADE, antibodies facilitate viral infection, thus amplifying infectivity and damage. Importantly, IP and ADE only develop during a recall immune response (16).

To address these questions, we thoroughly investigated the immune response to SARS-CoV-2 in a cohort of COVID-19 unvaccinated patients from the second wave in the Barcelona metropolitan area. The analysis showed that the serological responses and the trajectories of high-granularity lymphocyte clusters supported a recall immune response rather than a primary response. These recall immune response features are notably more prominent in moderate and severe cases than in mild ones.

RESULTS

Features of the Barcelona COVID second-wave cohort

The final cohort included 191 COVID-19 cases and 44 controls recruited in 2020, during the second wave of COVID-19 in Barcelona, before the vaccination campaign started in January 2021 (19). Of the patients, 38 were asymptomatic, 49 mild, 64 moderate, and 40 severe. The study's design is depicted in Figure 1. The inclusion criteria were being above 18 years of age, having a confirmed virological diagnosis of SARS-CoV-2 by PCR test, and agreeing to participate. In the case of healthy blood donors, in addition, the inclusion criteria were those of the blood bank, and the exclusion criteria were a history of an episode of COVID-19 or a positive serological test in our assay.

The initial plan was to collect samples the day entering the study and one and three weeks later; however, at that time, the health system was still overstretched, and the samples were collected at variable intervals, and not all patients contributed with three samples, i.e., of the symptomatic patients 107 patients contributed three samples, 34 two samples, and 12 one sample; controls and asymptomatic cases, they all contributed one sample as planned; a total of 483 samples were available for the study. For the analysis of results, we have used three periods based on the days from symptoms onset (DFSO), DFSO1 0-7 days, DFSO2 8-20 days, and DFSO3 21-60 days (with some samples collected up to 107 days). Due to delays in entering the health system, the first sample of 47 patients (26 moderate and 21 severe) was collected during DFSO2. The number of patients per period was 101, 128, and 60, and the number of samples per period was 139, 188, and 65, respectively. Of the 483 samples, only 13 (2.7%) were collected at DFSO >60. Due to financial constraints, cytokines were measured in 67 % and RNA profiles (Nanostring®) in 15% of the samples selected to represent each group. The period of controls and asymptomatic patients was annotated as DFSO_A and DFSO_C for data handling. The details of

the patient group, time course, and number of samples tested at each time point are represented in Figure 1, and all the details are in Table 1.

Out of the 106 hospitalized patients, 31 (29.2%) required admission to the ICU, and the median length of stay in the hospital (LOSH) was 15 days [7 - 25]. Their ICU stays averaged 14 days [7 -27]. The demographic, clinical, and laboratory data are in Tables 2 and 3. The overall mortality during the follow-up period was 6/191 (3.1%). The ages of the six deceased patients ranged from 68 to 80 years old.

ANALYSIS OF THE ANTIBODY RESPONSE TO THE SARS-CoV-2 PROTEINS

The time course profiles by isotype do not correspond to a typical primary immune response

We analyzed the serological response in 473 samples from 190 patients and 44 controls. The values were standardized using the control group's IQR3.

In period DFSO1, the antibody response showed significant differences in control versus all severity group patients, except for anti-RBD (Figure 2A and B). Interestingly, the only significant IgM response during this period was to the Spike protein. The differences became more evident in the following DFSO periods when the response to RBD and IgM isotype antibodies became detectable (see Supplemental Figure 1, A-D). Although the highest responses were initially observed in moderate patients, they became like severe patients during the follow-up and were not significantly different. Responses were also detected in asymptomatic patients but were only significant for anti-Spike IgG.

The antibody response was maintained for more prolonged in patients with more severe symptoms with a considerably later peak response, especially for anti-RBD and IgG isotype antibodies (Figures 3A and B). To better visualize the SARS-CoV-2 antibody response trajectories, we plotted severity-stratified data using LOESS smoothed regression that generated curves summarizing each isotype's antibody response. Two key observations emerged: 1) IgM responses did not appear before IgA or IgG, neither at the beginning nor at the peak of the response. 2) Antibody levels decreased in mild patients between 13 and 16 days but only after 30 and 47 days for moderate and severe patients.

This lack of an IgM response to SARS-CoV-2 preceding the IgG and IgA responses, as expected in an immune response to a new pathogen, suggested that in most patients, the response was, at least in part, a recall response. However, as in a LOESS regression, a few cases with a primary response can be missed; we looked for candidate primary responders by selecting patients who, during the initial seven days (n=139), had a normalized level of antibody above 1.5 for the IgM isotype and below 1.5 for the IgG or IgA isotype. The sum of Mpro, NP, and Spike antibodies for each isotype and patient was used for this filter. Eight cases (5.8%) were identified. They corresponded to four mild and four asymptomatic patients, all from the primary care sub-cohort, none requiring hospital admission (age 52 range 29-71, 5 females, and three males). Representative profiles are shown in Figure 3 D. The primary

responders developed good IgG and IgA antibody responses at period DFSO2, reaching titers similar to other cases of comparable severity (data not shown). The interpretation of these results is that in this COVID-19 cohort, the majority develop a recall type of immune response to SARS-CoV-2 proteins.

Antibody responses association with severity, mutual coordination, and correlation with cytokine are aligned with a recall immune response

A reported observation is that in COVID-19, the antibody response titer correlated with the disease's severity. In our cohort, higher antibody titers were associated with severity on the five-point scale (control, asymptomatic, mild, moderate, and severe; see material and methods), as seen in the pairwise comparison in Figure 2A, where titers are compared by severity and period. This observation is even more apparent when all cases are plotted with the maximum antibody titer (Figure 4A). This positive correlation was also found when severity was stratified by WHO scores, as shown in Supplemental Figures 2A and B).
The interpretation of the association of severity with the serological response is that antibodies do not protect against severity during the early stages of COVID-19, notwithstanding their protective role as RBD-neutralizing antibodies against re-infection (20).

An expected feature of a response to a new pathogen is a coordinated immune response to the pathogen's different antigens. In our cohort, the responses to the SARS-CoV-2 proteins are coordinated, but the response to RBD (Supplemental Figure 3, blue boxes). As the receptor binding domain (RBD) of SARS-CoV-2 differs significantly from other circulating coronaviruses, a delayed and slow response to RBD could indicate the need for a primary immune response distinct from the response to other SARS-CoV-2 proteins.

To identify which cytokines were driving the humoral response, we analyzed the correlations of cytokines with the antibody titers at each period and severity group. The most interesting observation is the significant negative correlation of IFN-γ, especially with the serological response in moderate patients at DFSO2; it is known that there is a mutual inhibitory effect of IFN-γ/IL-2 and IL-4/IL-13 in the initial polarization of the immune response, which may explain these results (21) (Supplemental Figures 4). The positive correlation of IL-7 with antibody titers in severe and moderate patients is probably due to IL-7 being secreted to compensate for lymphopenia, which correlates negatively with antibodies to SARS-CoV-2 (22). Overall, the pattern of cytokines in moderate and severe cases suggests a mixture of early and late secondary immune responses.

ANALYSIS OF THE CELL POPULATIONS IN COVID-19 PATIENTS

Changes in the main leukocyte populations

As reported, neutrophils were relatively expanded in COVID-19 patients, and lymphocytes were relatively reduced (8). To better analyze B and T cell populations, we have used either the absolute number or the proportion of a subset within one of the lymphocyte main compartments. Low T lymphocytes, monocytes, and NK cells were detected during the initial DFSO1 period. The most significant changes were observed in plasma cells, which increased in all cases (Supplemental Figure 5).

High-dimensional flow cytometry produced a hi-granularity landscape of lymphocyte subset changes associated with SARS-CoV-2 infection.

The flow cytometric analysis of fresh total blood resolved 46 populations split into 197 clusters. For the interpretation, three degrees of resolution were considered: low (7 subsets), like that typically used in clinical flow cytometry, medium as in use in advanced clinical flow cytometry units (46 cell subsets); and high (197 clusters), a level in which the physiological and clinical interpretations of many clusters is still uncertain. The mutual correlations of these populations at each time point and for each clinical group have been analyzed. Only those contributing to discern between a primary and a recall response are included in this report.

Trajectories of plasmablast subsets show features of a recall response

Plasmablasts and plasma cells, from here on PBs, as defined by CD38 +, CD27+, HLA-DR++, sIg, and variable CD19, were split into four main clusters: IgA+, IgG+, IgM+, and sIg^- and three low-abundance clusters: IgM+IgA+, IgM+IgG+, and long-life plasma cells (LLPC), as seen in the uniform manifold approximation and projection plot (UMAP) (Figure 5A and B).

The number of PBs rose rapidly in moderate and severe patients, surpassing already at DFSO1 day three the maximal levels of mild patients at day 7; moreover, their maximal number of plasmablast exceeded the maximal number in mild patients by a factor of 2 and 3 respectively (Figure 5 C). In some severe and deceased patients, PBs made up to 60% of lymphocytes (Supplemental Figure 6A). Analysis of the PB subsets, total number, and proportion over the total PB indicated that IgA+ PB was the dominant subset during the incubation period, which was then replaced by sIg- PB at DFSO1 day 3 (Figure 5 D and E). The trajectory of precursor B cells increasing before the rise in serological titers suggests that these cells are the source of at least some of the antibodies to SARS-CoV-2 (Figure 5F). The correlation between sIg^- PB number and anti-SARS-CoV-2 antibodies in mild patients at DFSO1 supports this trend

(Supplemental Figure 6B). The correlation with cytokines was investigated to understand better the mechanism of PB relative expansion (Supplemental Figure 7). A negative correlation with type 1 cytokines IFN-gamma and IL-2 and a positive correlation with IL-10 and IL-7 was observed, consistent with an ongoing immune response.

Interpretation: The first IgA plasmablasts probably originate from upper airway mucosa SLO. Given the magnitude, dynamics, and short incubation time of COVID-19(23), they are more likely to result from memory B cells specific to the cross-reactive CCCV virus than a fast primary response.

Trajectories of the B lymphocyte subset in COVID-19 patients are consistent with a recall response

High-resolution spectral flow cytometry identified 32 clusters of B lymphocytes summarized in 13 subsets and eight unclassified minor clusters (Figure 6A and Supplemental Figure 8). The Total B cell trajectory is distinct from that of leukocytes and T cells, but peaks and valleys show parallelism (Figure 8B). Subset trajectories are very variable (Figures 6, D-H); switched and memory subset trajectories differed markedly among severity groups and also when compared by period and severity (See Supplemental Table 2. B cell subset statistics).

The B cell subset correlation analysis with the serological response revealed a distinct pattern. In mild patients, the correlations are positive during the initial eight days (DFSO1), significant for B cell subsets involved in the early phase of the response, i.e., transitional, naïve activated, IgM-only memory, and CD24++ immature IgG memory (Figure 7A and Supplemental Figure 9 for high-resolution B cell clusters). In moderate and severe, this correlation is clearly detected in DFSO2

Consistently, the trajectories of memory and switched subsets show a delay in the regression curves (Figure 7B) and when analyzed by periods in the rings plot (Figure 7C).

Interpretation: The overall cell dynamic is consistent with a recall response. The capture of antigens by CCCV memory B cells may delay trajectories in moderate and severe cases. A fresh specific response to SARS-CoV-2 is initiated only when a large amount of antigen reaches the secondary lymphoid organs.

Trajectories of cTfh cells in COVID-19 patients are consistent with recall response.

Circulating Tfh (cTfh) reflects the activity of Tfh cells in secondary lymphoid organs (SLO) (24–26). It correlates with antibody response, but the trajectory differs from total T cells or typical effector memory CD8 cells (Figure 8A). cTfh, as Tfh, can be classified as cTfh-naïve, cTfh1, cTfh17, cTfh2, and cTfh1 activated (26), as identified in the T cells UMAP (Figure 8B). All clusters were significantly higher in asymptomatic and mild than moderate and severe (Figure 8C). Among all T cell subsets, cTfh

is the subset whose cell number is significantly more reduced when comparing moderate or severe patients vs. mild ones. This association of cTfh reduction with severity was not explained by age in a multivariable model corrected for age. Notably, despite their low number of cTfh cells, the rise in antibodies to SARS-CoV-2 is earlier and faster in moderate and severe patients than in mild patients, suggesting that they are produced by memory B cells (Figure 8A). CXCR5, the defining cTfh marker, was higher in asymptomatic and mild patients than in moderate and severe patients, indicating recent egress from SLO in these patients (Supplemental Figure 8A). The high positive correlations in the cTfh clusters to serological response analysis confirm that Tfh participates in the antibody response (Supplemental Figure 8B).

Interpretation: The overall pattern of cTfh response aligns with a recall response, but the differences among severity groups could be due to modulation by immune priming.

Nanostring transcriptomic signature

Seventy samples from 33 patients, representative in terms of age, sex, and severity, were selected for transcriptomic profiling. The results were stratified for the analysis in 60 gene groups.

The strong BCR signaling signatures in asymptomatic patients are of interest because other techniques detected only relatively changes in this group (Figure 9). In the Immune memory panel, the stronger signal for CD45RA in asymptomatic and mild patients with the differential pattern in the lymphocyte trafficking highlights the different regulation of the immune responses in asymptomatic and mild vs the hospitalized moderate and severe. It is also remarkable that there is an interferon response signature in the asymptomatic and some mild cases. These results confirm a gene expression pattern consistent with an immune response, mainly recall.

The panels of genes associated with myeloid and monocyte cell activation and the expected IL-1 signaling show some of the main differences related to severity (Supplemental Figure 11).

These results are similar to many transcriptomic profiles of COVID-19 patients and indicate that our cohort is representative of COVID-19 (27–29).

Discussion

At the start of the COVID-19 pandemic, it was appreciated that around 20% of the patients developed pneumonia, many of which required oxygen therapy and intensive care unit admission. Many attempts were made to generate predictive algorithms that would help triage patients and support the management of the crisis. In fact, most predictive algorithms relied heavily on the clinical signs of severity, therefore not anticipating severity but rather confirming it (8, 30).

One possible determinant of severity is the existence of immunological memory to CCCV antigens that cross-react with SARS-CoV-2 antigens at the B and T cell levels and enhance or interfere with the immune response to SARS-CoV-2, the mechanism designated as antigenic imprinting (IP) or original antigenic sin. This possibility has been discussed (31, 32) and there is evidence that most individuals possess antibodies (33) and memory T cells (31, 34) to CCCV that cross-react with SARS-CoV-2 proteins, including a contemporary study in the Barcelona area population (35). A recent study also establishes a link between pre-existing immunity to CCCV immunity and severity (36). Pre-existing immunity to CCCV may be protective or detrimental depending on the localization of the cross-reactive epitopes, the type of memory, and the coexisting determinants of severity in a given patient. In spite of this evidence, IP as determinant of COVID-19 severity has not become an accepted paradigm.

There is a lack of studies focused on whether the immune response to SARS-CoV-2 is primary or recall and whether there is an association between the type of response and severity; of note, only a recall response can be associated with IP.

In this paper, we report that the trajectories of antibody responses to SARS-CoV2, when analyzed in detail, together with the clinical course and the trajectories of plasmablasts, B cell and cTfh indicate that in 131 out of 139 (94.3%) cases, the immune response to SARS-CoV-2 is a, at least in part, a recall response. The features of recall response were more evident in the two categories of patients that required hospitalization. The implication is that being the immune response to SARS-CoV-2 a recall response in the majority of cases, IP may be a major modulator of SARS-CoV-2 infection.

In our study, clinical data were curated by the physicians in charge of the patients and not just downloaded from the electronic clinical records of the health provider; patients were all from the same geographical area and from a single health provider (Institut Català de la Salut (ICS), https://ics.gencat.cat) that ensures similar standard of care and includes patients from a broad spectrum socio-economic status. The control group, voluntary healthy blood donors, were recruited in parallel to the patients. On the technical side, flow cytometry was carried out on fresh blood samples immediately analyzed which probably aided to preserve better activated cell subsets; cytokines were measured by Biotechne® microfluidic technique implemented in the service laboratory during the previous three years and proven very robust; transcriptomic data were obtained by Nanostring®, a technology which does not include a PCR based amplification. All these methodological aspects make the data particularly robust.

Our analysis was triggered by the simple observation that in our cohort IgM responses to SARS-CoV-2 antigens did not precede the IgG and IgA responses as expected. In fact, in the first 2020 reports of

antibody response to SARS-CoV-2, this anomaly was already detected, but the focus was on applying serology to diagnosis (9, 10, 37, 38)

A close analysis of the antibody response trajectories by SARS-CoV2 protein and isotype, stratified by patients' severity, offers additional cues of a recall immune response. The fast and dominant IgA responses to the Mpro, NP, and Spyke suggest a mucosal origin from memory resident T (Trm) and B cells in the mucosa of the upper airways (39–41). That the IgM response, even if weaker, is dominated by the response to Spike, which is the protein whose sequence is more different from that of endemic seasonal coronaviruses, suggests the recruitment of naïve cells, even if late, contributes to mounting a response to SARS-CoV-2 specific epitopes. The vigorous but delayed IgG response may originate from deeper lymph nodes draining the lower respiratory airways. The response to RBD is challenging to analyze, probably due to the much smaller antigen size used in the detection assay. It is, however, noteworthy to point out that we detected a robust late IgG response to RBD in moderate and severe patients. Another, not mutually exclusive, possibility is that SARS-CoV-2 Spike can engage memory and naïve lymphocytes in the mucosa where tissue damage generates more PAMP and jump-starts the immune response. All the above is consistent with the concept that in COVID-19, a recall response to antigens cross-reactive with CCCV coexists with a response to new epitopes in the SARS-CoV-2 Spyke protein.

One major limitation of our study is that we did not measure antibodies to endemic coronavirus in samples obtained before and after the COVID-19 episode. Unfortunately, this failure is due to the initial design of the study aimed at improving the definitions of the immunotypes identified in our previous study (42). However, contemporary studies in the same populations demonstrated a high prevalence of antibodies to endemic coronavirus in these populations (35). Another limitation is that we did not test the sera for neutralizing SARS-CoV-2 antibodies, but it has been repeatedly shown that they correlate closely with anti-RBD antibodies (43).

Antigenic original sin, as the negative side of the immune imprinting, may have harmful consequences for the host. The predominant immune response is directed to the dominant epitopes of the prior immunizing strain of the pathogen, and the effectors generated, antibodies and T cells, having low affinity for the new epitopes, are inefficient, resulting in a more severe infection (44). The cellular and molecular basis is well understood; memory B and T cells capture the cross-reactive protein, and as they have a lower threshold for activation, they dominate the response, preventing the activation of naïve cells that carry more specific receptors for the new epitopes. However, as medium affinity antibodies and T cells may have some protective effect and eventually, as the amount of viral antigens reaching the lymph nodes increases, a primary specific response may later emerge, takes over, and leads

to the control of the infection. However, besides interfering with the primary response, the original antigenic sin can be associated with an even more damaging mechanism: antibody-dependent enhancement (ADE). Repeatedly observed in viral infections, e.g., dengue, and occasionally after vaccination (18), it is attributed to macrophage infection via Fc and complement receptors and, consequently, dissemination of the virus and to the polarization of macrophages towards the M2 phenotype (45). The participation of this mechanism in COVID-19 has been discussed, and it has been a concern in developing the SARS-CoV-2 vaccines (46).

The observations in our study and others (14, 32–35, 46–52) that suggest an element of OAS in COVID-19 can be summarized as:

1) The lack of preceding IgM responses in most cases.

2) The quick fall and short life of antibody response is, a feature of IP (16).

3) The response to RBD that is particularly delayed and subject to large interindividual variability.

4) The correlation of SARS-CoV-2 titers with disease severity supports the contention that the antibody response contributes to severity rather than resolution of the infection; this would fit with a response is directed in part to epitopes cross-reactive with CCCV.

5) Plasmablast levels increase much more significantly in the more severe categories, reminiscent of dengue at second exposure (53).

6) The preferential expansion of surface-negative plasmablasts suggests memory B cells in the mucosa and deep SLO ready to be mobilized as pre-plasma cells (54).

7) The features of B cell subsets profiles and of cTfh and their correlation with the antibody responses are consistent with a recall response.

In conclusion, upon analyzing the trajectory of a set of immunological variables during the acute episode of COVID-19, we can infer that immunological memory plays a significant role in influencing the response to SARS-CoV-2. The evidence that in the majority of patients the response to SARS-CoV-2 is a recall response reinforces the contention the previous exposure to endemic coronavirus is through IP a major determinant of COVID-19 outcome yet to be fully appreciated (14, 36, 50).

COROLLARY

Based on the above and the ample literature on OAS in COVID-19, we can figure out the scenarios that lead to the different severity categories.

1. In asymptomatic and mild patients, there is some but less interference by prior immunity to CCCV, so patients mount an efficient immune response; as they are mostly young, they have a diverse T and B naïve repertoire; this may explain the higher affinity (despite lower titer) of antibodies in asymptomatic and mild patients (55).

2. In moderate patients, memory B and T cells interfere more with the immune response in the SLO, which delays the generation of antibodies and specific cytotoxic T cells. Eventually, the memory cells expand and control the infection with a variable contribution of newly recruited naïve cells.

3. In severe and critical cases, the operating mechanism may be similar to moderate ones, as demonstrated by their similar T and B cell subsets and cytokines profiles. Still, an element of ADE is added to this scenario as delayed high-titer antibodies— and possible T effector T cells— of low affinity find abundant viral protein in the alveoli and generate a strong local hypersensitivity reaction.

In summary, if the adaptive immune response to SARS-CoV-2 is usually a recall response, IP and ADE may explain the "misfiring" of the immune response to COVID-19 in patients requiring hospitalization (14, 31–35, 47, 48, 56).

METHODS

Patients

The cohort of patients participating in the study was recruited by the attending physicians of the participating hospitals (hospital Universitari Bellvitge (HUB), Hospital Universitari Germans Trias I Pujol, (HUGTP); Hospital Universitari Vall d'Hebron (HUVH) upon admission or at primary care centers during the first contact. In the latter scenario, a team of nurses visited patients' homes, collected clinical data, and obtained blood samples. Detected asymptomatic household sharing cases were recruited. All participants were duly informed of the project's objectives and signed the corresponding consent forms approved by the institutional ethical review boards. Blood samples were collected into citrate, EDTA, sera separation, and Tempus® tubes (Becton-Dickinson Inc, NJ, USA). Samples were

planned to be obtained on days 0, 5, and 15. Volunteer donors from blood banks healthy SARS-Cov-2 uninfected donors who declared not being aware of at least one episode of COVID-19 were recruited by the Blood and Tissue Bank of Catalonia (BST, www.bst.cat); however, three of these donors had to be excluded because serology indicated a previous episode of asymptomatic COVID-19.

A Research Electronic Data Capture (REDCap) database (57, 58) was designed to collect clinical and laboratory data. Data were introduced in 182 fields, which include 15 for demographic and identification details, 22 for medical treatment history, 19 for comorbidities, the Charlson and SOFA indexes, 37 for initial symptoms, vital signs, and physical examination, 46 for follow-up information including oxygen requirements and therapy, and 31 for general clinical chemistry data, IL-6, and calprotectin. The clinical data and blood samples were collected at the beginning and at two more time points, except for controls and asymptomatic patients, whose data were only collected once. For all patients, the date of symptom onset was recorded and used to calculate "days from symptom onset" (DFSO) for each observation. The length of hospital stay (LOS), ICU stay, oxygen supplementation, and ventilation support were also documented.

Clinical severity categories were determined by the highest score during the follow-up period using the World Health Organization (WHO) 8-point COVID-19 disease clinical progression score (59). The scores correspond to phenotypic categories: 0 no clinical or virological evidence of infection, 1: no limitation of activities, 2: limitation of activities, not requiring hospitalization, 3: hospitalized without oxygen requirement, 4: oxygen administered via a mask or nasal prongs, 5: non-invasive ventilation or high-flow oxygen, 6: intubation and mechanical ventilation, 7: ventilation and additional organ support (vasopressors, renal replacement therapy, ECMO), and 8: deceased. In many analyses, patient classification was simplified as asymptomatic (score 1), mild (score 2), moderate (score 3-4), and severe (score of 5 to 8). Deceased patients were sometimes separated from those classified as severe. Moderate and severe patients were all hospitalized.

Clinical Laboratory Tests

SARS-CoV-2 was detected by a real-time multiplex RT-PCR assay (Laplet 2019-nCoV Assay, Seegene, South Korea) in samples from nasal or pharyngeal swabs. Microbiological and clinical chemistry samples were processed by automatic analyzers integrated into continuous lines with automatic cold storage that ensured sample integrity.

Immunological Tests

Cytokines and related proteins

The levels of CCL2, CXCL10, GM-CSF, IFN-α, IFN-γ, IL-2, IL-4, IL-6, IL-7, IL-10, IL-12p70, IL-13, IL-15, IL-17A, TGF-β1, TNF-α, granzyme-B and IL-1RA were measured in sera using the ELLA microfluidic platform (Biotechne®, Minneapolis, MN, USA). Calprotectin was measured by CLIA (Quantaflash®, Werfen, Barcelona, Spain).

SARS-CoV-2 serology

Antibodies of the three immunoglobulin isotypes IgM, IgG, and IgA against SARS-CoV-2 main protease (M^{pro}), nucleocapsid (NP), Spike (S) protein, and the RBD portion of the Spike protein were measured in serum samples at each time point of patient follow-up and from one sample of the control and asymptomatic group patients using a commercial kit (SARS-COV-2 MULTIPLEX®, IMMUNOSTEP, Salamanca, Spain), for more details see ref (60). Inactivated serum samples were incubated with magnetic polystyrene beads coated with SARS-CoV-2 recombinant proteins. The M^{pro} and NP antigens were produced in E. coli, while the full-length S protein (residues 1 to 1208) or its RBD (residues 332 to 534) were produced in HEK-293F cells. Binding was then revealed with isotype-specific conjugated antibodies and acquired in a Navio flow cytometer (Beckman-Coulter Inc., Brea, CA).

In some analyses, the sum of antibody levels for each isotype to M^{pro}, NP, and S proteins were used to score each individual's overall isotype-restricted response to SARS-CoV-2, annotated as SARS-CoV-2 IgA, SARS-CoV-2 IgG, and SARS-CoV-2 IgM.

High-dimensional flow cytometry

Whole blood was processed as detailed in (61). RBC lysis was the first step, and there was no density gradient separation. Cells were stained with a 36-color antibody panel (Supplemental Table 1) and analyzed using a 5-laser Aurora spectral flow cytometer (Cytek Biosciences, CA). During the development of the panel, adjustments were applied to avoid artifacts, e.g., non-specific staining was detected between anti-IgG, anti-TCR Vδ2, and anti-IgA antibodies due to the binding of anti-IgG antibodies to both TCRVδ2 and IgA. The original protocol was modified staining for TCRVδ2 and IgA after fixation, which improved their signal. Samples were processed and analyzed within 6 hours (61). Unsupervised statistical inferences of the data were computed by OMIQ data analysis software

(www.omiq.ai), UMAP was utilized for dimensionality reduction, and flow SOM for clustering, resulting in multiple 46 populations and 197 clusters (see Results) (61).

Transcriptomic profiling by Nanostring

For Nanostring profiling, 250 ng of total RNA from PBMC, quantified using the NanoDrop 2000 (Thermo Scientific), was directly hybridized (at 65°C for 18 h) with a mixture of biotinylated capture probes and fluorescently labeled reporter probes complementary to target sequences. After solution-phase hybridization between target RNA and reporter-capture probe pairs, excess probes were washed away using a two-step magnetic bead-based purification on the nCounter Prep Station. Finally, the RNA/Probe complexes were aligned and immobilized in the cartridge for data collection. The cartridge was transferred to the nCounter Digital Analyzer for image acquisition and count collection. Gene expression values were first normalized to the positive controls and then normalized to the geometric mean expression of the 12 housekeeping genes included in the panel (ABCF1, ALAS1, GUSB, HPRT1, MRPS7, NMT1, NRDE2, OAZ1, PGK1, SDHA, STK11IP and TBP -1), according to nCounter Expression Data Analysis Guide (mAN-C0011-02). The nCounter® Human Immunology Host Response Panel was used for this study (https://nanostring.com/products/ncounter-assays-panels/immunology/host-response/).

Statistical analysis

Analysis was conducted in the R environment version 4.3.1 using R Studio with packages tidyverse, rstatisx, ggpubr, and broom (https://cran.r-project.org). The distribution of all variables was tested for normality (Shapiro test), and non-parametric tests were applied to analyze those not normally distributed. All tests considered two-tailed distributions to calculate the p-value, which was adjusted using the Bonferroni method, except when stated otherwise, p values <0.05 were considered significant. In LOESS smoothed regression curves, 95% CI are represented unless otherwise stated.
The analysis was carried out by the bioinformatic and statistical analysis unit of Vall Hebron Research Institute (https://vhir.vallhebron.com/ca/suport-la-recerca/unitat-destadistica-i-bioinformatica-ueb), ASP, R.P-B and DAS

ETHICAL

The institutional ethics board approved this project of the three institutions (HUVH: Protocol number PR(AG)242/2020, HUGTP, and HUB.

DATA AVAILABILITY

Supplemental tables contain the additional data required to re-analyze the data: the xlsx file with the transcriptomic data will be made available on request.

AUTHOR CONTRIBUTION

D. A-S, M. M-G, A. S-M, J. B-M, A. T-S, M. H-G, and R. P-B conceived and designed the project based on previous collaborations and maintained the project activity and logistics during the pandemic. A. S-M designed the redcap database to collect all clinical information, M.A. F-S and H. A performed the high-dimension flow cytometry data analysis and interpretation. J.A.E-P., E.P-C. C. Z-E, F.M-R, and B. U-V collected samples and clinical data from hospitalized patients, while C.V. organized the collection of samples and clinical data from the primary care centers and visiting nurses' teams. R.P. collected the samples and data from the volunteer blood donors that constituted the control group. A. S-P. designed and performed part of the statistical and bioinformatic analysis. E.M-C., M. M-G, and C.V. reviewed and contributed to several draft versions of the manuscript. P.K. reviewed the pre-final versions critically and suggested insightful new analyses included in the final version. A.V. carried out the Nanostring analysis and data interpretation. D. A-S ran the project and performed the cytokine analysis and parts of the statistical and bioinformatic analysis. R.P-B ran the project, carried out the global data analysis and interpretation, wrote the manuscript, and generated most tables and figures.

ACKNOWLEDGMENTS

This study was funded by Instituto de Salud Carlos III, Madrid, Spain, grants COV20/00416, Cov20/00654, and COV20/00388 to RP-B, AT-S, and JB-M respectively, and co-financed by the European Regional Development Fund (ERDF). D.Á-S is the recipient of a doctoral fellowship from the Vall Hebron Research Institute, Barcelona, Spain (up to 2022 and a postdoc fellowship "Sara Borrell," CD23/00114 (from 2024). A.S-M was supported by a postdoctoral grant, "Juan Rodés" (JR18/00022), from Instituto de Salud Carlos III through the Ministry of Economy and Competitiveness, Spain. Bioinformatics analysis has been carried out in parte in the Statistics and Bioinformatics Unit (UEB) at Vall d'Hebron Research Institute (VHIR).

The authors thank all the patients and health staff of the Hospital Universitari Vall d'Hebron, Hospital Universitari Bellvitge, and Hospital Universitari Germans Trias i Pujol and Primary Care Units who endured the pandemic and did their best to overcome the successive waves of COVID-19 in Barcelona, an experience that none of us would ever forget. The authors are grateful to Sergio Navarro Velázquez and Mario Framil Seoane from Hospital Universitari Bellvitge and to Arturo Llobell Uriel and Joan Roig Sanchis from Hospital Universitari Vall d'Hebron for their support in reviewing patients' records within the general Immuno-profile COVID-ICS project. Dr Isabel Novoa-Garcia and Ms. Sheyla Pascual Martin for their invaluable help in organizing and maintaining the COVID-19 collection in the HUVH BioBank. To Ms Adelaida Parada and the administrative and technical staff of immunology laboratories at the participating hospitals that collected and organized the COVID-19 patient samples for review by the medical personnel of this study.

REFERENCES

1. Steiner S, et al. SARS-CoV-2 biology and host interactions. *Nat Rev Microbiol*. 2024;1–20.

2. Davis HE, et al. Long COVID: major findings, mechanisms and recommendations. *Nat Rev Microbiol*. 2023;21(3):133–146.

3. Li X, et al. Clinical determinants of the severity of COVID-19: A systematic review and meta-analysis. *PLoS ONE*. 2021;16(5):e0250602.

4. Zhang Q, et al. Inborn errors of type I IFN immunity in patients with life-threatening COVID-19. *Science*. 2020;370(6515):eabd4570.

5. Su HC, et al. Interfering with Interferons: A Critical Mechanism for Critical COVID-19 Pneumonia. *Annu Rev Immunol*. 2023;41(1):561–585.

6. Bastard P, et al. Autoantibodies against type I IFNs in patients with life-threatening COVID-19. *Science*. 2020;370(6515):eabd4585.

7. Initiative TC-19 HG, et al. A second update on mapping the human genetic architecture of COVID-19. *Nature*. 2023;621(7977):E7–E26.

8. Sánchez-Montalvá A, et al. Exposing and Overcoming Limitations of Clinical Laboratory Tests in COVID-19 by Adding Immunological Parameters; A Retrospective Cohort Analysis and Pilot Study. *Front Immunol*. 2022;13:902837.

9. Long Q-X, et al. Antibody responses to SARS-CoV-2 in patients with COVID-19. *Nat Med*. 2020;26(6):845–848.

10. Li K, et al. Dynamic changes in anti-SARS-CoV-2 antibodies during SARS-CoV-2 infection and recovery from COVID-19. *Nat Commun*. 2020;11(1):6044.

11. Murphy K, Weaver C. Integrated dynamics of innate and adaptive immunity. *Janeway's Immunobiology*. New York and London: Garland Science, Taylor & Francis Group; 2017:445–491.

12. Racine R, Winslow GM. IgM in microbial infections: Taken for granted? *Immunol Lett*. 2009;125(2):79–85.

13. Duan Y, et al. Deficiency of Tfh Cells and Germinal Center in Deceased COVID-19 Patients. *Curr Méd Sci*. 2020;40(4):618–624.

14. Rijkers GT, Overveld FJ van. The "original antigenic sin" and its relevance for SARS-CoV-2 (COVID-19) vaccination. *Clin Immunol Commun*. 2021;1:13–16.

15. Francis T. On the Doctrine of Original Antigenic Sin. *Proceedings of the American Philosophical Society*. 1960;104(6):572.

16. Yewdell JW, Santos JJS. Original Antigenic Sin: How Original? How Sinful? *Cold Spring Harb Perspect Med*. 2020;11(5):a038786.

17. HALSTEAD SB, O'ROURKE EJ. Antibody-enhanced dengue virus infection in primate leukocytes. *Nature*. 1977;265(5596):739–741.

18. KIM HW, et al. Respiratory Syncitial Viurs Disease in Infants Despite Prior Aministration of Antigenic Inativated Vaccines. *Am J Epidemiology*. 1969;89(4):422–434.

19. Andrés C, et al. A year living with SARS-CoV-2: an epidemiological overview of viral lineage circulation by whole-genome sequencing in Barcelona city (Catalonia, Spain). *Emerg Microbes Infec*. 2022;11(1):172–181.

20. Goldblatt D, et al. Correlates of protection against SARS-CoV-2 infection and COVID-19 disease. *Immunol Rev*. 2022;310(1):6–26.

21. Sun J, Pearce EJ. Suppression of Early IL-4 Production Underlies the Failure of CD4 T Cells Activated by TLR-Stimulated Dendritic Cells to Differentiate into Th2 Cells. *J Immunol*. 2007;178(3):1635–1644.

22. Fry TJ, Mackall CL. The Many Faces of IL-7: From Lymphopoiesis to Peripheral T Cell Maintenance. *J Immunol*. 2005;174(11):6571–6576.

23. Lauer SA, et al. The Incubation Period of Coronavirus Disease 2019 (COVID-19) From Publicly Reported Confirmed Cases: Estimation and Application. *Ann Intern Med*. 2020;172(9):M20-0504.

24. Morita R, et al. Human Blood CXCR5+CD4+ T Cells Are Counterparts of T Follicular Cells and Contain Specific Subsets that Differentially Support Antibody Secretion. *Immunity*. 2011;34(1):108–121.

25. Vinuesa CG, et al. Follicular Helper T Cells. *Annu Rev Immunol*. 2016;34(1):1–34.

26. Crotty S. T Follicular Helper Cell Biology: A Decade of Discovery and Diseases. *Immunity*. 2019;50(5):1132–1148.

27. Ren X, et al. COVID-19 immune features revealed by a large-scale single-cell transcriptome atlas. *Cell*. 2021;184(7):1895-1913.e19.

28. Schulte-Schrepping J, et al. Severe COVID-19 Is Marked by a Dysregulated Myeloid Cell Compartment. *Cell*. 2020;182(6):1419-1440.e23.

29. Wang X, et al. Temporal transcriptomic analysis using TrendCatcher identifies early and persistent neutrophil activation in severe COVID-19. *JCI Insight*. 2022;7(7). https://doi.org/10.1172/jci.insight.157255.

30. Wynants L, et al. Prediction models for diagnosis and prognosis of covid-19: Systematic review and critical appraisal. *The BMJ*. 2020;369. https://doi.org/10.1136/bmj.m1328.

31. Dykema AG, et al. Functional characterization of CD4+ T-cell receptors cross-reactive for SARS-CoV-2 and endemic coronaviruses. *J Clin Investig*. 2021;131(10). https://doi.org/10.1172/jci146922.

32. Aguilar-Bretones M, et al. Impact of antigenic evolution and original antigenic sin on SARS-CoV-2 immunity. *J Clin Investig*. 2023;133(1):e162192.

33. Anderson EM, et al. Seasonal human coronavirus antibodies are boosted upon SARS-CoV-2 infection but not associated with protection. *Cell*. 2021;184(7):1858-1864.e10.

34. Mateus J, et al. Selective and cross-reactive SARS-CoV-2 T cell epitopes in unexposed humans. *Science*. 2020;370(6512):89–94.

35. Aydillo T, et al. Immunological imprinting of the antibody response in COVID-19 patients. *Nat Commun*. 2021;12(1):3781.

36. McNaughton AL, et al. Fatal COVID-19 outcomes are associated with an antibody response targeting epitopes shared with endemic coronaviruses. *JCI Insight*. 2022;7(13). https://doi.org/10.1172/jci.insight.156372.

37. Suhandynata RT, et al. Longitudinal Monitoring of SARS-CoV-2 IgM and IgG Seropositivity to Detect COVID-19. *J Appl Lab Med*. 2020;5(5):908–920.

38. Verkerke H, et al. Comparison of Antibody Class-Specific SARS-CoV-2 Serologies for the Diagnosis of Acute COVID-19. *J Clin Microbiol*. 2021;59(4):e02026-20.

39. Gregoire C, et al. Viral infection engenders bona fide and bystander subsets of lung-resident memory B cells through a permissive mechanism. *Immunity*. 2022;55(7):1216-1233.e9.

40. Oja AE, et al. Trigger-happy resident memory CD4+ T cells inhabit the human lungs. *Mucosal Immunol*. 2018;11(3):654–667.

41. Grau-Expósito J, et al. Peripheral and lung resident memory T cell responses against SARS-CoV-2. *Nat Commun*. 2021;12(1):3010.

42. Mueller YM, et al. Stratification of hospitalized COVID-19 patients into clinical severity progression groups by immuno-phenotyping and machine learning. *Nat Commun*. 2022;13(1):915–915.

43. Suthar MS, et al. Rapid Generation of Neutralizing Antibody Responses in COVID-19 Patients. *Cell Rep Med*. 2020;1(3):100040.

44. Baumgarth N. Original antigenic sin: not so sinful after all. *Trends Immunol*. 2023;44(7):487–489.

45. Taylor A, et al. Fc receptors in antibody-dependent enhancement of viral infections. *IMMUNOLOGICAL REVIEWS*. 2015;268(1):340 364.

46. Lee WS, et al. Antibody-dependent enhancement and SARS-CoV-2 vaccines and therapies. *Nat Microbiol*. 2020;5(10):1185–1191.

47. Aguilar-Bretones M, et al. Seasonal coronavirus-specific B-cells with limited SARS-CoV-2 cross-reactivity dominate the IgG response in severe COVID-19 patients. *J Clin Investig*. 2021;131(21). https://doi.org/10.1172/jci150613.

48. Johnston TS, et al. Immunological imprinting shapes the specificity of human antibody responses against SARS-CoV-2 variants. *Immunity*. 2024;57:912-925.e4.

49. Shrock E, et al. Viral epitope profiling of COVID-19 patients reveals cross-reactivity and correlates of severity. *Science*. 2020;370(6520):eabd4250.

50. Tetro JA. Is COVID-19 receiving ADE from other coronaviruses? *Microbes Infect*. 2020;22(2):72–73.

51. Thomas S, et al. Antibody-Dependent Enhancement (ADE) and the role of complement system in disease pathogenesis. *Mol Immunol*. 2022;152:172–182.

52. Woudenberg T, et al. Humoral immunity to SARS-CoV-2 and seasonal coronaviruses in children and adults in north-eastern France. *EBioMedicine*. 2021;70:103495.

53. Kwissa M, et al. Dengue Virus Infection Induces Expansion of a CD14+CD16+ Monocyte Population that Stimulates Plasmablast Differentiation. *Cell Host Microbe*. 2014;16(1):115–127.

54. Vijay GKM, Singh H. Cell fate dynamics and genomic programming of plasma cell precursors. *Immunol Rev*. 2021;303(1):62–71.

55. Hendriks J, et al. High Titers of Low Affinity Antibodies in COVID-19 Patients Are Associated With Disease Severity. *Front Immunol*. 2022;13:867716.

56. Lucas C, et al. Longitudinal analyses reveal immunological misfiring in severe COVID-19. *Nature*. 2020;584(7821):463–469.

57. Harris PA, et al. Research electronic data capture (REDCap)—A metadata-driven methodology and workflow process for providing translational research informatics support. *J Biomed Inform*. 2009;42(2):377–381.

58. Harris PA, et al. The REDCap consortium: Building an international community of software platform partners. *J Biomed Inform*. 2019;95:103208.

59. WHO. R&D Blueprint novel Coronavirus, COVID-19 Therapeutic Trial Synopsis. Appendix 1 [preprint]. 2020.

60. Cáceres-Martell Y, et al. Single-reaction multi-antigen serological test for comprehensive evaluation of SARS-CoV-2 patients by flow cytometry. *Eur J Immunol*. 2021;51(11):2633–2640.

61. Fernandez MA, et al. Single-Cell Protein Analysis, Methods and Protocols. *Methods Mol Biology*. 2022;2386:C1–C3.

Figures and legends to figures

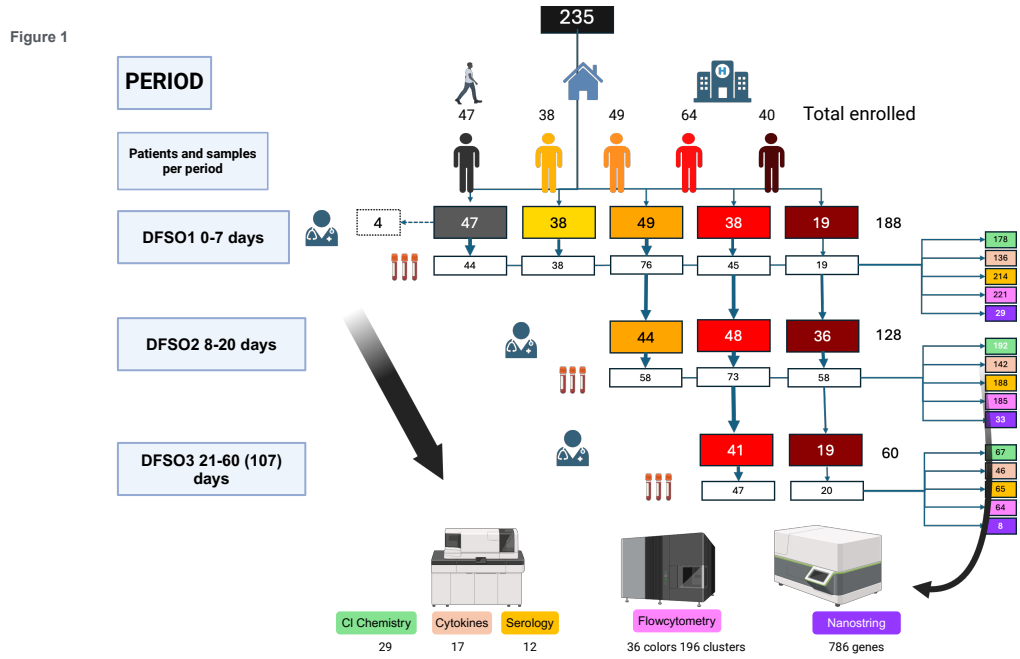

Figure 1. Study design and patient flow chart. The figure summarizes the patient groups, the timeline, and the number of variables measured in each group. Clinical data were available from all 235 individuals, but due to financial limitations, cytokine and Nanostring tests were applied to approximately 60-70 % and 20% of the samples, respectively (see text). DFSO, days from symptoms onset; Asympt, asymptomatic cases, see text in section "Features of the Barcelona COVID second-wave cohort" of results for details.

Figure 2

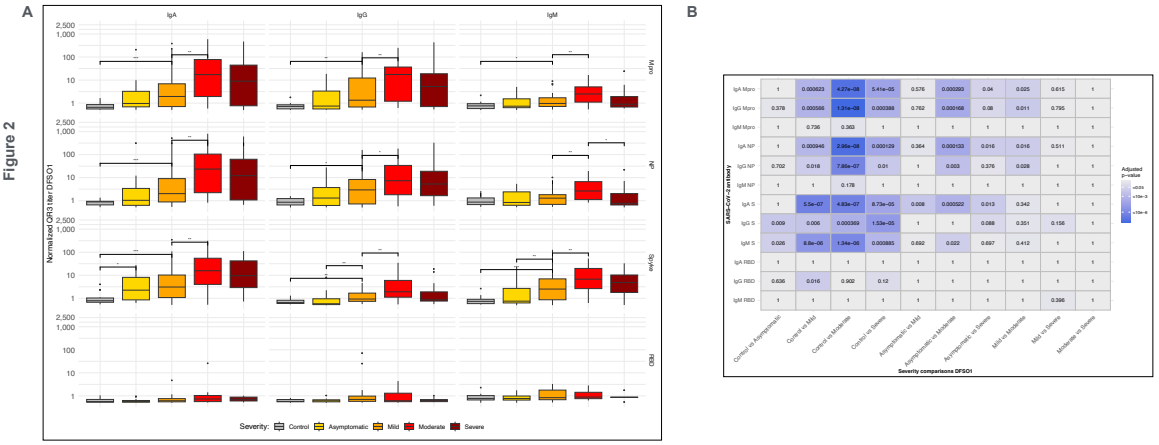

Figure 2. Pairwise comparison of antibody response to SARS-CoV-2 proteins in the different groups of patients. (**A**) The plots correspond to the 0-7 days from symptom onset (DFSO1), only significant different among adjacent boxplots and to controls are annotated. (**B**) *p* values for each possible comparison from (A); cells with p values >0.05 are not painted. Paired Wilcox test, adjusted *p* values. The corresponding graphics for periods DFSO2 and DFSO3 are in Supplemental Figure 1.

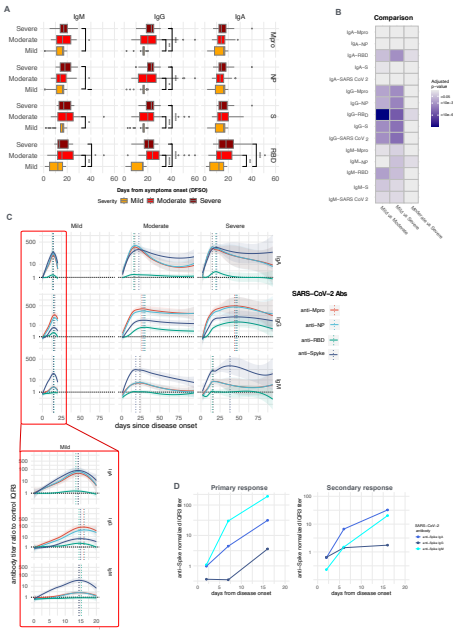

Figure 3. Trajectories of SARS-CoV-2 antibody levels. (A) The peak levels of the 88 cases from which we collected three samples during the initial 60 days, are plotted against time. There's a noticeable delayed peak for moderate and severe cases compared to mild cases. (B) A heatmap summarizes the significance level of the comparisons, highlighting clustering in the IgG category and the comparison between mild vs. severe and mild vs. moderate cases. (C) LOESS regression curves with 95% confidence intervals of the normalized antibody titers of 392 samples from 190 COVID-19 cases are shown. The vertical dotted lines represent the maximal titer, and the horizontal lines represent the established normal level for data normalization. In the red box inset, the time scale has been zoomed to visualize the trajectories during the initial 20 days. It's highlighted that the first response is IgA, followed by IgG and IgM. The responses have already started to decrease at 13-15 DFSO. The rise of the IgM antibody regression curve never precedes the other isotype curves in moderate or severe patients. The maximal IgG titer is reached between 43 and 47 days for moderate and severe patients. It's also noteworthy that the predominant antigen for IgM isotype antibodies is Spike, while IgA, NP, Mpro, and NP predominate over Spike for IgG. Responses to RBD were predominantly IgG. (D) Representative patients for primary and secondary responses; only responses to Spike have been represented.

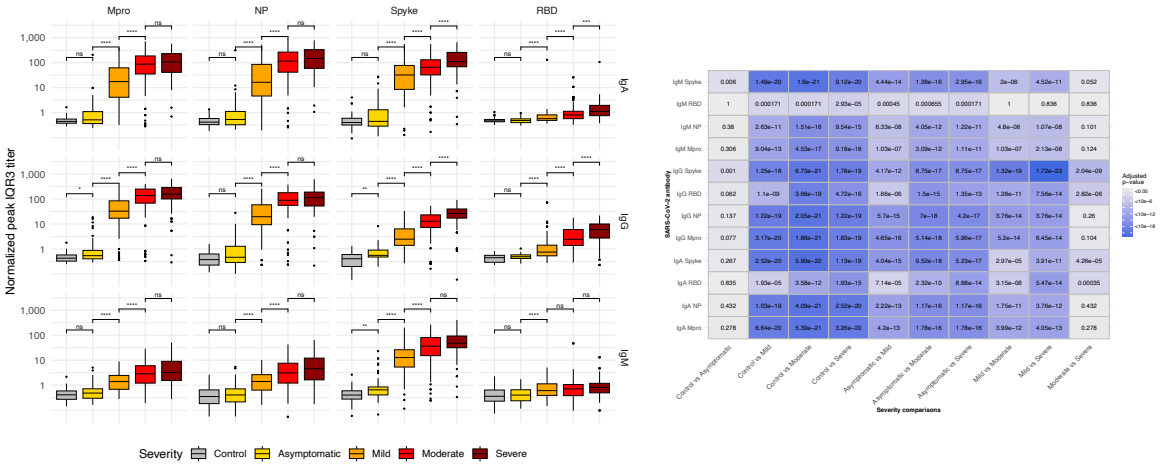

Figure 4. The intensity of the antibody response increases with severity. (A) Maximal antibody levels for the clinical 100 cases with three serological measurements plus control and asymptomatic cases compared. Notice how the antibody levels significantly increase with the severity. (B) Heatmap summarizing plot comparisons, Pairwise Wilcoxson test. See supplemental Figure 2 for the same analysis but with the WHO eight-point scale.

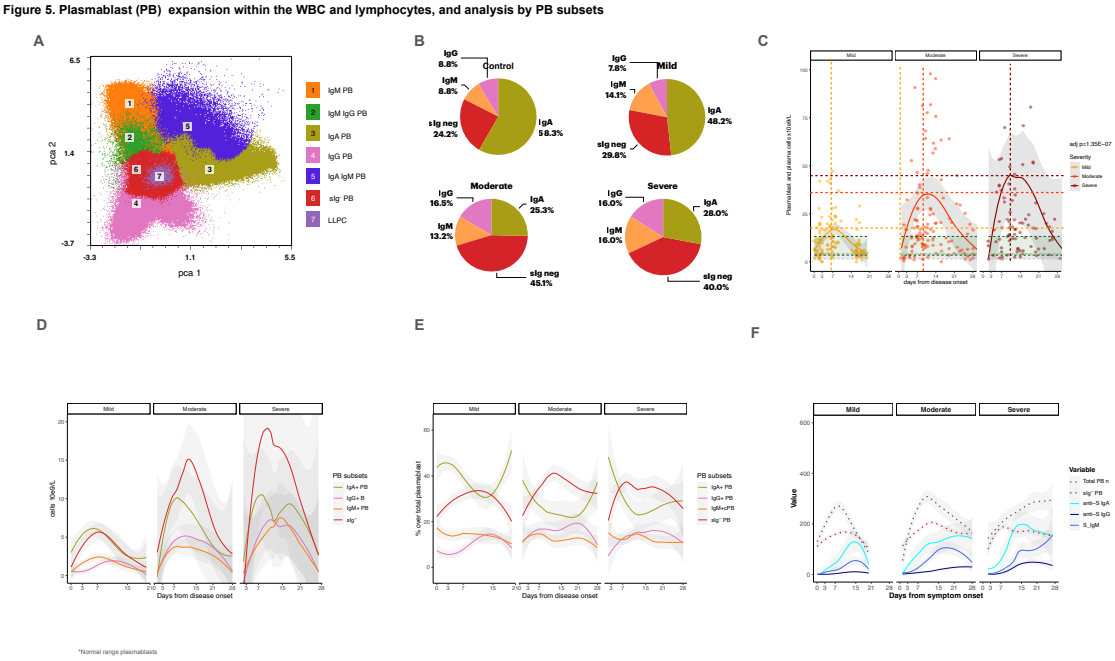

Figure 5. Plasmablast (PB) expansion within the WBC, lymphocyte populations, and plasmablast (PB) subset analysis. (A) UMAP of plasmablast clusters; (B) Distribution of plasmablast among the four main subpopulations, IgA+, IgG+, IgM+, and sIg^- in controls and the three severity categories. The expansion of PB is due to the rise in the number of sIg^- PBs. (C) Trajectories of total plasmablasts during the initial 28 days by severity categories. The horizontal dashed lines point at the different levels of the maximal number of cells. The vertical dashed lines indicate the day the maximal level is reached for each category highlighting the remarkable differences in their respective trajectories. The magnitude of PB's absolute expansion can be appreciated; (D) The comparison of the proportions of the most abundant PB subsets over total PB reveals that this expansion is primarily due to the increase in sIg^- PB. (E) Proportion of PB subsets over total PBs. (F) Composite plot showing total PBs and sIg- PB trajectories and normalized antibody titers to SARS-CoV-2 S proteins. Values in the Y-axis are either cell numbers or normalized antibody titers, but cell numbers have been transformed to place them in the same range as serological titer

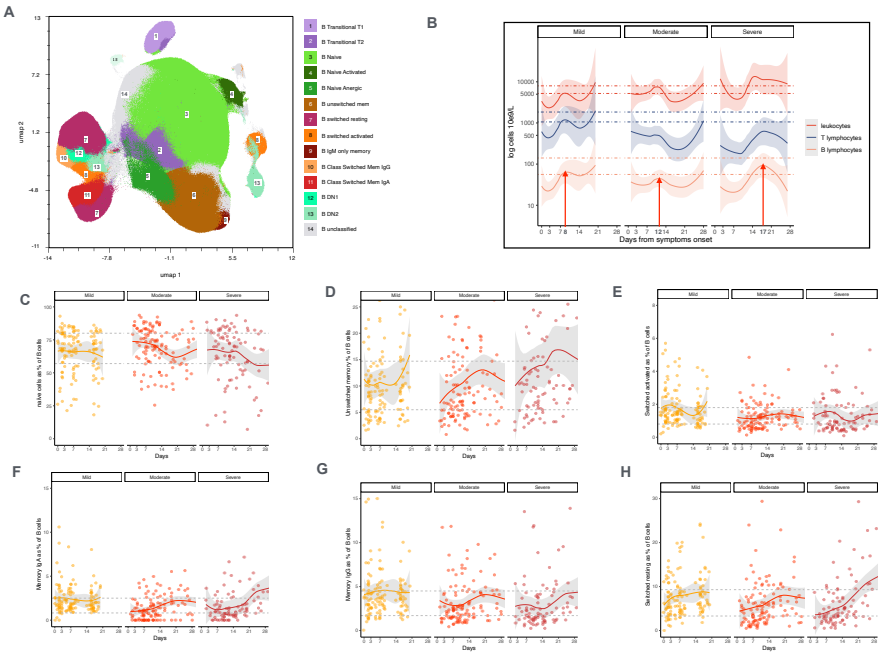

Figure 6. Trajectories of B cell subsets. (A) UMAP of B cells displays the distribution of the 13 subpopulations that summarized 32 clusters. (B) LOESS line of leucocytes, T and B lymphocytes count trajectories for the three categories of clinical COVID-19 cases. In plots C-H, the number of samples is. As follows: mild 130, moderate 134, and severe 89. The y-axis represents the percentage of total B cells. (C) Naïve; (D) unswitched memory; (E) Switched activated; (F) Memory IgA; (G) Memory IgG; (H) switched resting B cells. The dashed lines indicate quartiles 1 and 3 of the distribution of the values in the control population for each subpopulation. By comparing each population (C-H) with (B), it is noticeable that the circulating B cell population is less reduced compared to total lymphocytes and that recovery is earlier in the less severely ill patients.

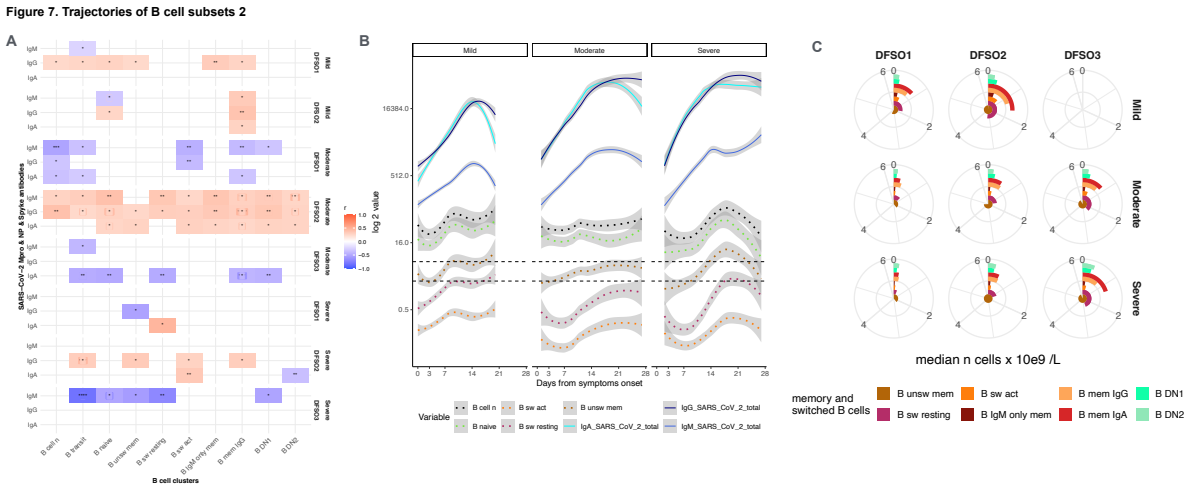

Figure 7. **Trajectories of B cell subsets associated with a recall immune response. (**A) Heatmap summarizing the correlation (Spearman) of B cell subsets and serological response by severity and follow period. DFSO, days from symptoms onset. DFSO1 0-7. DFSO2 8-20, DFSO3 21-107. (B) LOESS regression trajectories comparing B cell subsets and antibodies to SARS-CoV-2 proteins. (C) Ring pie charts comparing the distribution of the B cell subset along the follow-up period by severity. See text for details. Notice that the inner circles represent the most abundant subpopulations.

Figure 8

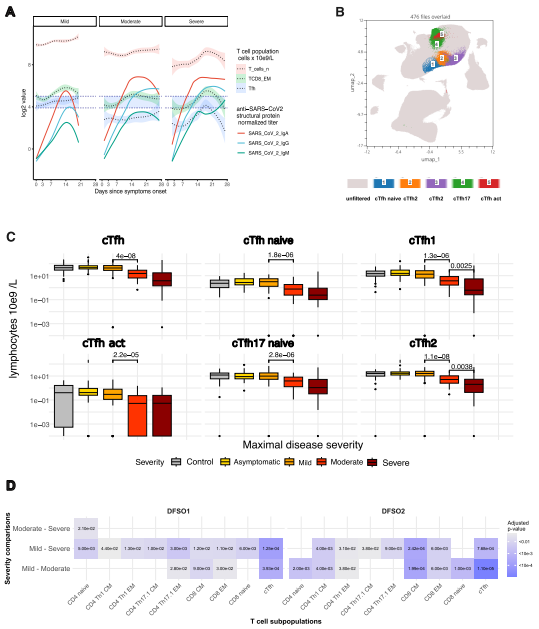

Figure 8. cTfh and clusters. (A**)** Comparison of LOESS trajectories of total T lymphocyte number, CD8 EM, and cTfh with the trajectories of normalized antibody to SARS structural proteins. The 95% CI of trajectories is represented; the blue ribbon helps to visualize how cTfh in mild remains consistently above the levels in moderate and severe patient groups. Notice that in moderate and severe, the antibody titers rise despite a lower number of cTfh. (B) UMAP shows the distinct cTfh clusters within the T cell distribution. (C) Both total Tfh (top left panel) and each cTfh subcluster have significantly different values distributions for mild vs moderate (Wilcoxon test p. adjust Benjamin-Hochberg). (D) Heatmap showing the pairwise comparison of T cell subsets among the severity groups. cTfh distribution is the most significantly different (Wilcoxon test p. adjust Benjamin-Hochberg).

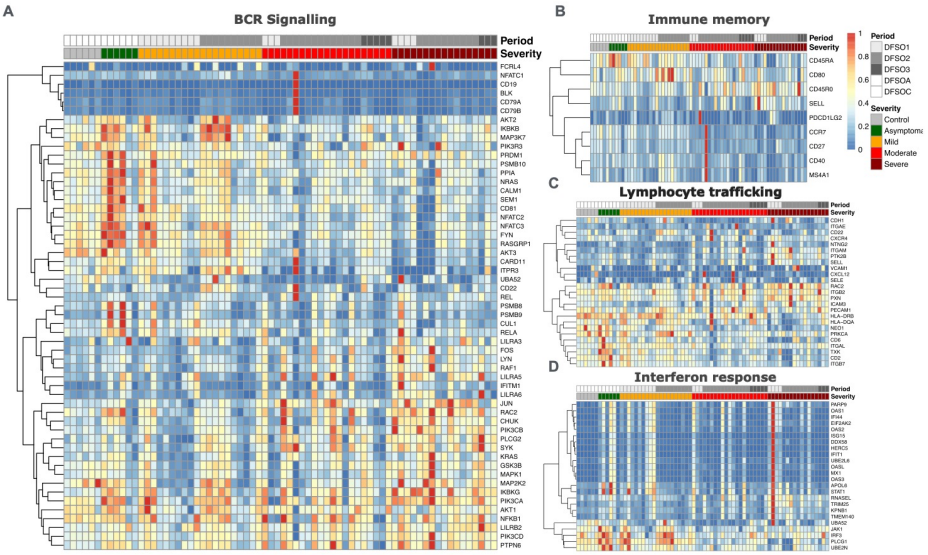

Figure 9. Heatmaps summarizing the transcriptomic profile of 33 COVID-19 patients stratified by severity and follow-up periods. (A) BCR signaling group of genes; (B) Immune memory; (C) Lymphocyte Trafficking; and (D) Interferon signaling.

Legends to Supplemental figures

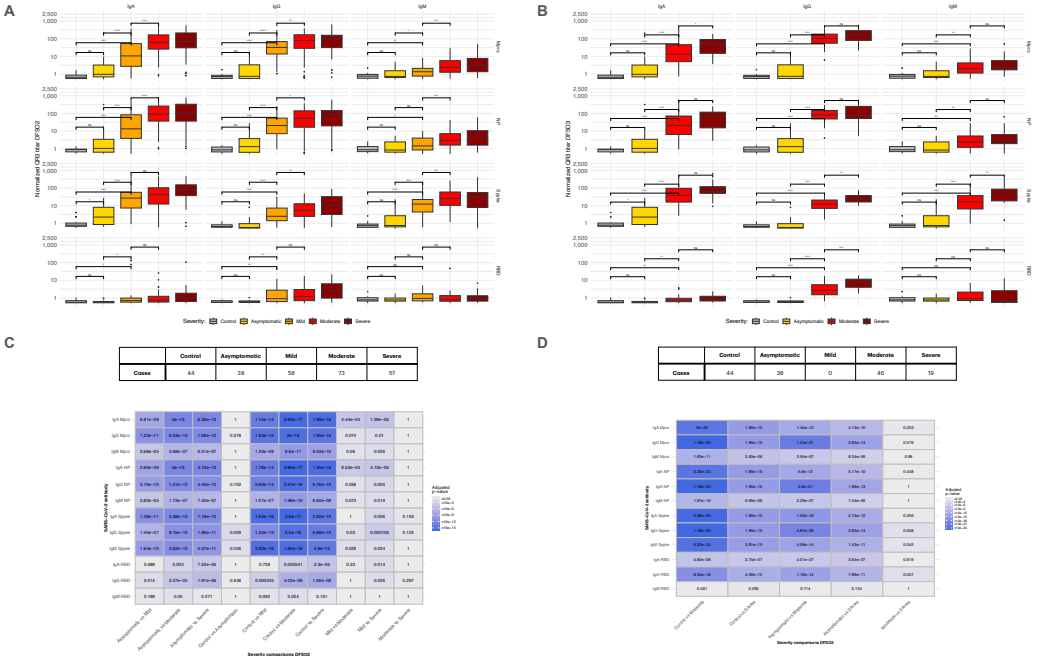

	Control	Asymptomatic	Mild	Moderate	Severe
Cases	44	38	56	73	57

	Control	Asymptomatic	Mild	Moderate	Severe
Cases	44	38	0	46	19

Supplemental Figure 1. Pairwise comparison of antibody response to SARS-CoV-2 proteins in the different groups of patients. (**A**) and (**B**) Plots corresponding to the 8-20 days period (DFSO2) from symptom onset and 0-107 days (DFSO3). (**C**) and (**D**) Tables with the number of cases in each category and adjusted *p* values for each possible comparison from (**A**) and (**B**). Pairwise Wilcoxon rank sum test. The corresponding graphics for period DFSO1 are in Figure 1.

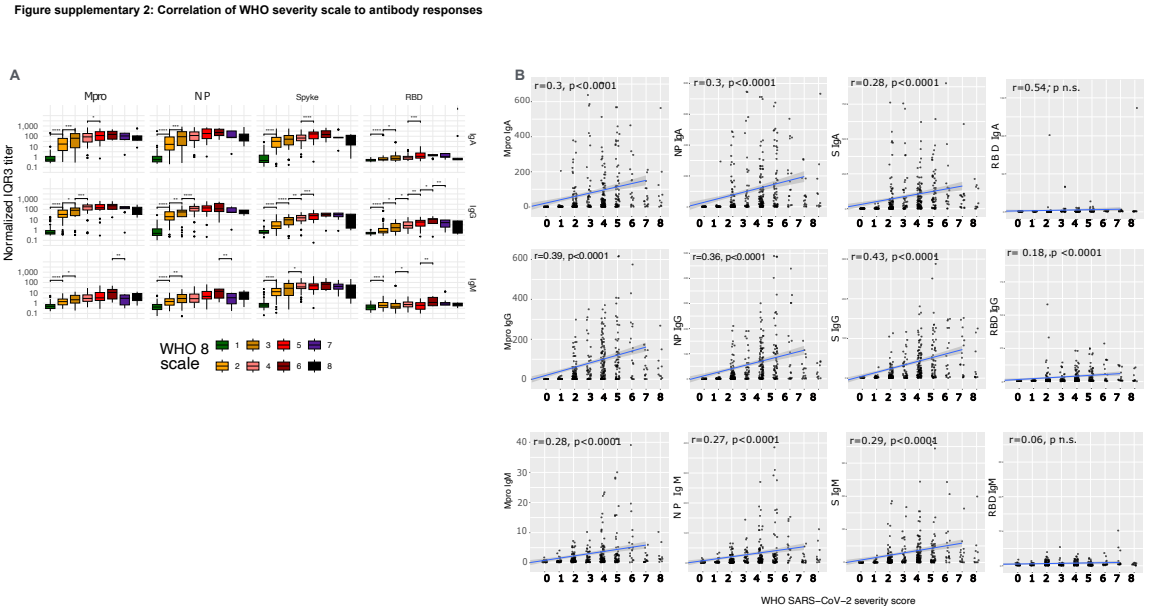

Supplemental Figure 2: SARS-CoV-2 antibody titers and WHO severity scale. (**A**) Only significant differences to the adjacent groups are annotated in box plot severity group comparisons. (B) Panels of linear correlation analysis for each antibody to SARS-CoV-2 proteins. X-axis WHO classification has been used as a continuous variable for this analysis. Y-axis normalized antibody titers. Notice that all correlations are positive, but only anti-S IgG severity shows an r>0.4; the correlation does not extend beyond category 6; critically ill patients had lower antibody levels.

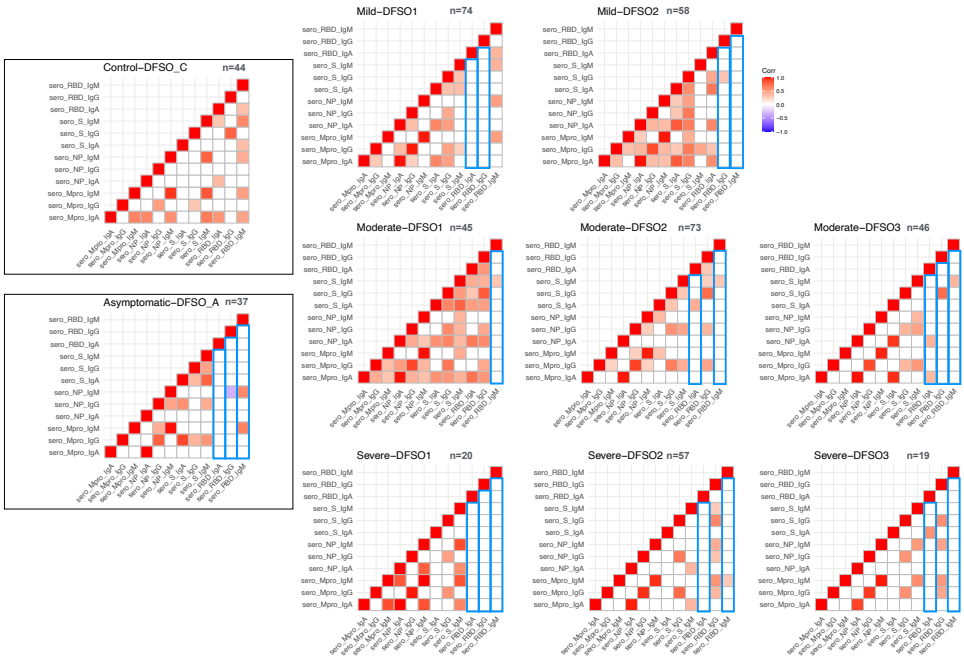

Supplemental Figure 3. Mutual correlation among the antibody responses to SARS-CoV-2 by antigen and Ig isotype stratified by severity and time (Spearman). The ten panels show mutual correlations; the number of patients is indicated in the upper right corner of each panel. DFSO, days from symptoms onset; DFSO1: 0-7, DFSO2:8-20, DFSO3: 21-107. In addition, DFSO_C corresponds to controls, and DFSO_A corresponds to asymptomatic. Maximal mutual correlations are seen in the mild and moderate panels, and correlations increase in severe patients at the late time point. RBD is mostly dissociated, highlighted by the blue boxes.

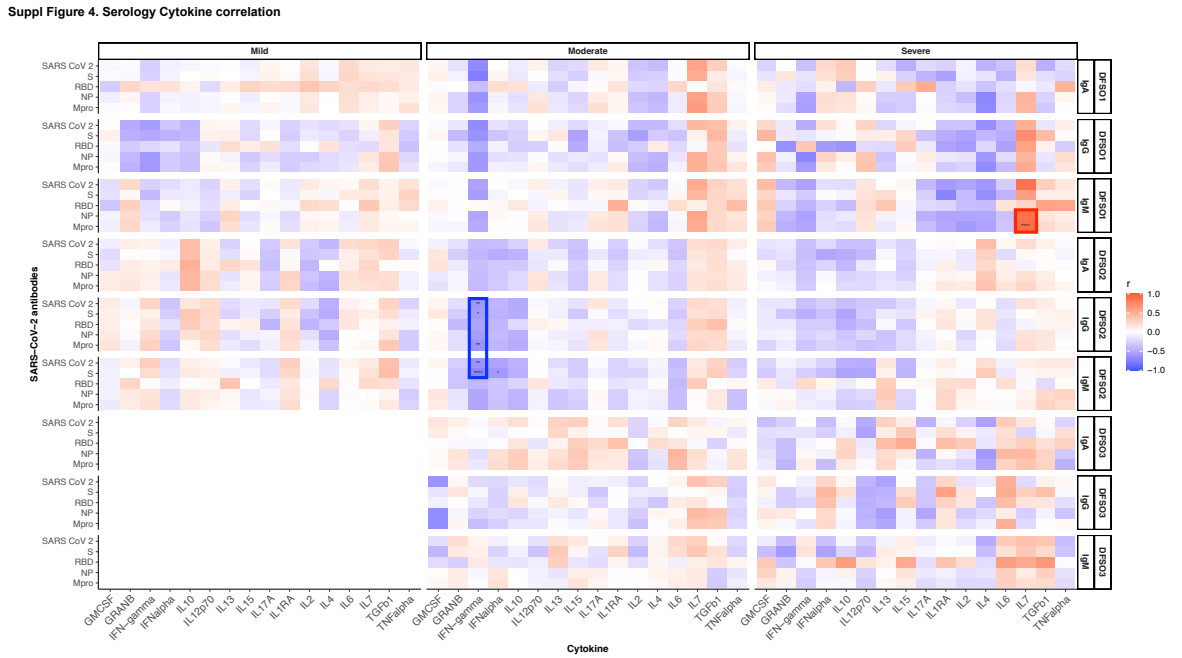

Supplemental Figure 4: Correlation among the antibody responses to SARS-CoV-2 by antigen, Ig isotype, and cytokines stratified by severity and time. Data from 309 samples corresponding to 159 representative cohort cases were available. There is a negative correlation of IFNs, especially gamma, with the serological response (blue box). Correlation of IL-7 to serological response (red box), see text for the interpretation.

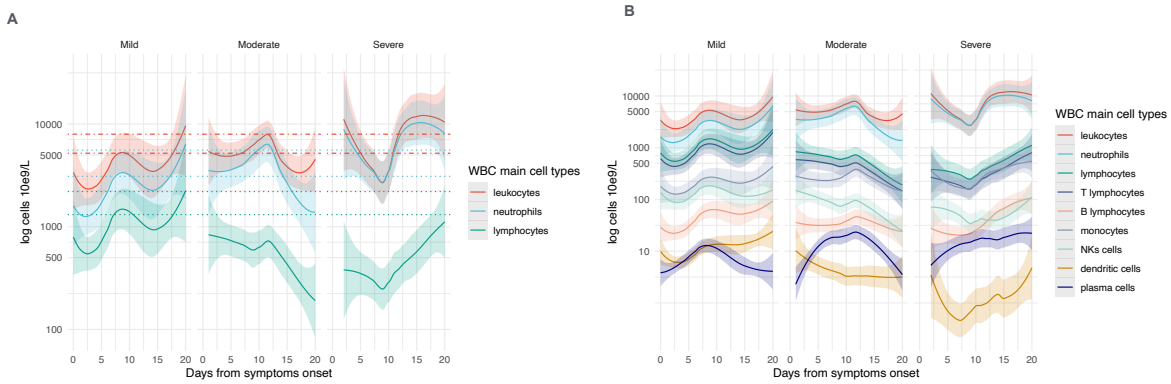

Supplemental Figure 5. Trajectories of the main differential white blood cell counts by severity groups during the initial 20 days. The lines represent values averaged by LOESS regression of 326 samples collected before day 20; the number of samples by severity group was 133 Mild, 155 Moderate, and 78 Severe. The CI has been adjusted to 0.75 to reduce overlaps. The y-axis is on a log scale, but the labels correspond to the number of cells; values from controls IQR 0.25 – 0.75 are indicated by horizontal dots or dash lines that maintain the color code. In (A), the three main types are plotted; nine populations are plotted in (B) to compare the trajectories.

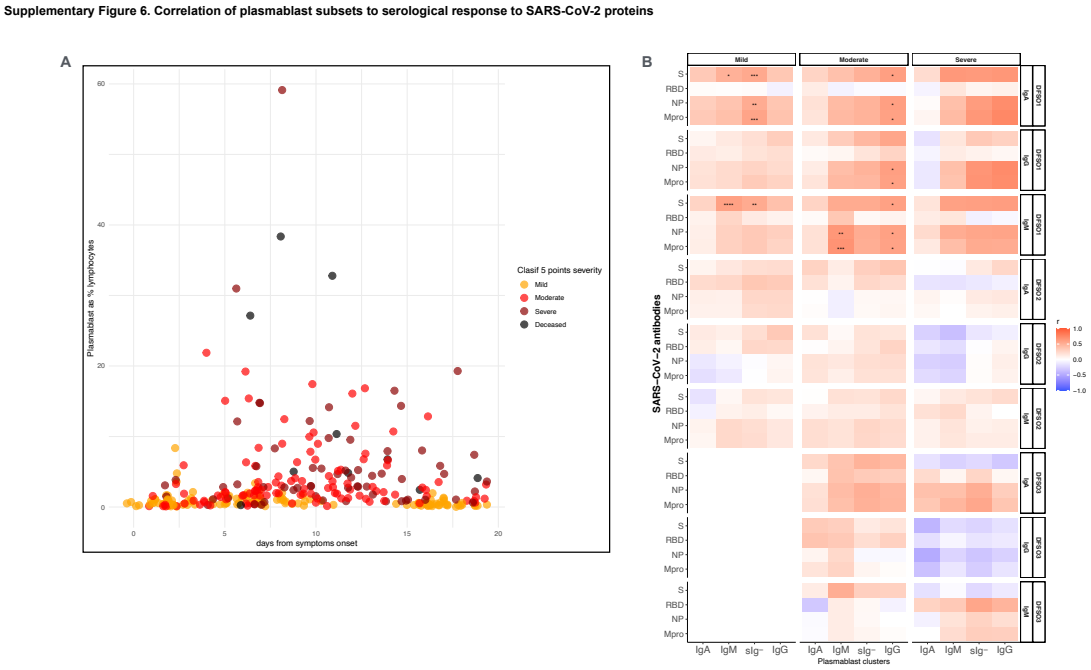

Supplemental Figure 6. Plasmablast (PB). (**A**) Dot plot showing the percentage of total PBs in the cohort of symptomatic COVID-19 patients during the initial 20 days of follow-up. Extreme values of up to 60% of the lymphocytes are observed in severe and deceased extremely lymphopenic patients. (B) Distribution of subsets in PB from controls in which total PB makes only 0.16 [0.09 - 0.27] % of the lymphocytes.

Suppl Figure 7 Plasmablast cytokines

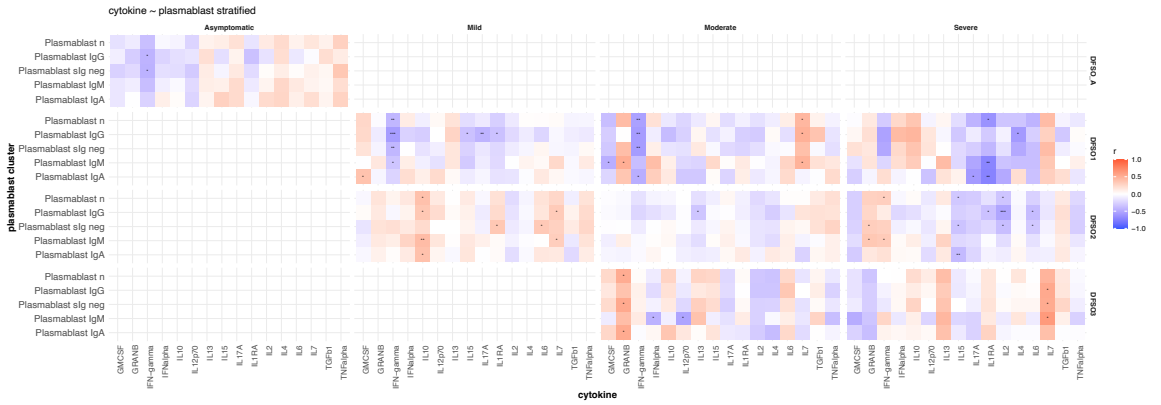

Supplemental Figure 7. Correlation of cytokines with plasmablast subsets. DFSO, Days from symptom onset. DFSO1, samples collected between 0-7 days; DFSO2, samples collected between 8-28 days; DFSO3, samples collected between 28-107 days. See text for comments. Adjusted *p* values p <0.05=*, $p < 0.01$=**, $p < 0.001$=***, $p < 0.0001$****, p not adjusted. See comments in the text.

Supplementary Figure 8

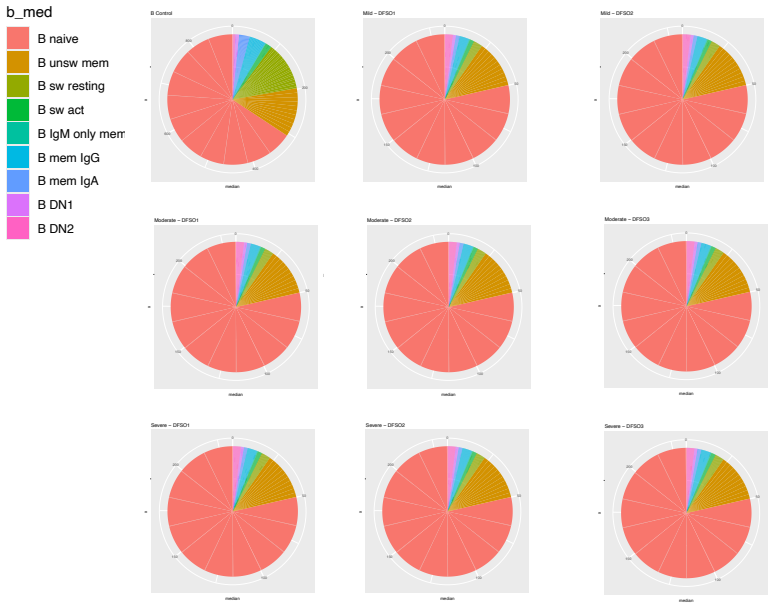

Supplemental Figure 8. Distribution of B cell subsets in controls and patients. A set of pie plots shows the changes in the distribution of B cells among the different subsets during the COVID-19 time-course. Notice that B cell switched resting is the only population showing a major reduction.

Supplementary Figure 9

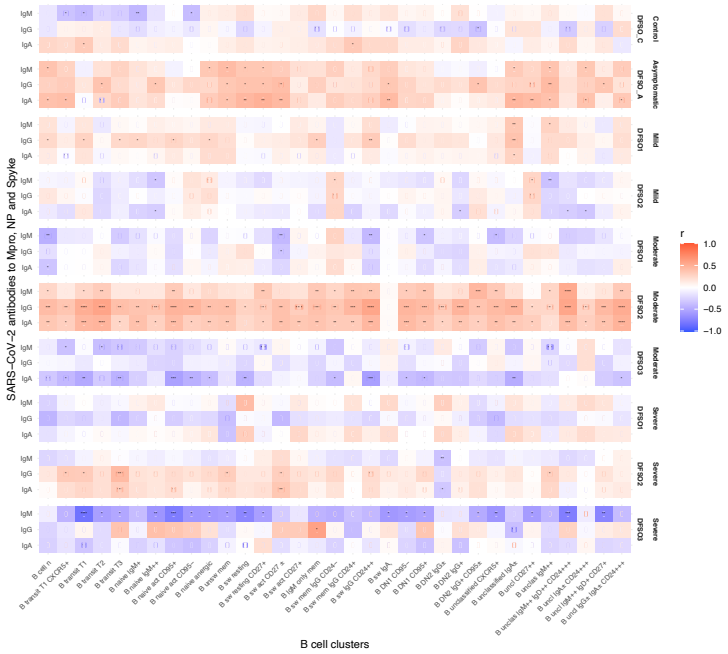

Supplemental Figure 9. Correlation of B cell cluster and serological response. DFSO_C and DFSO_A period during which control and asymptomatic patients' samples were collected; DFSO1, samples collected between 0-7 days; DFSO2, samples collected between 8-28 days; DFSO3, samples collected between 28-107 days. See text for comments. Adjusted *p*, $p < 0.05$=*, $p < 0.01$ =**, $p < 0.001$=***, $p < 0.0001$ = ****. See comments in the text.

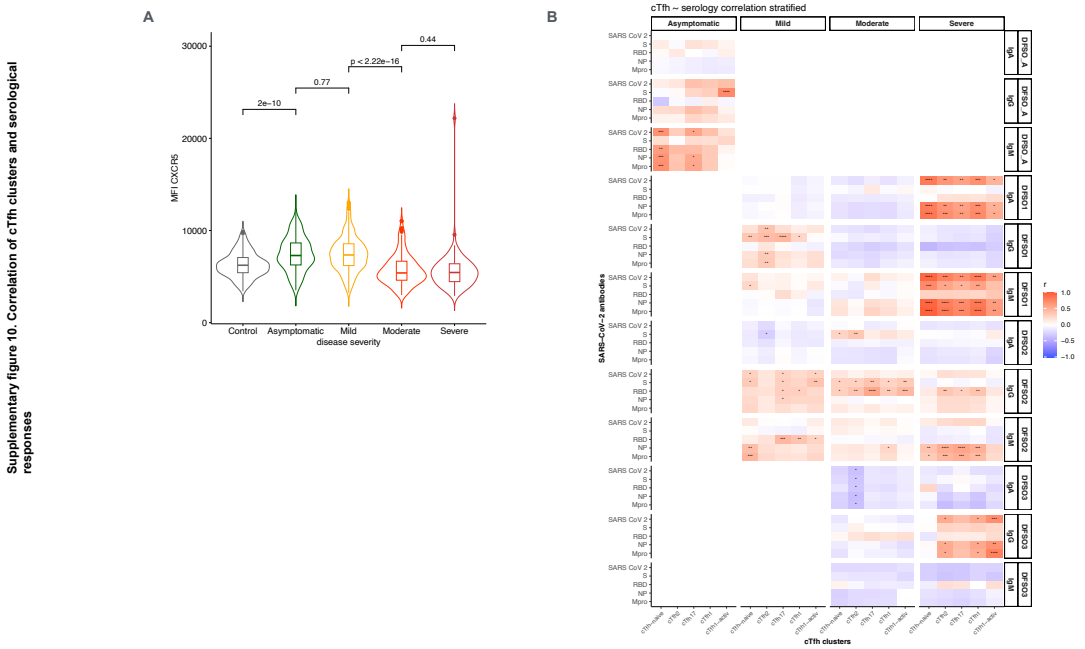

Supplemental Figure 10. cTfh and serological response (Spearman). (A) CXCR5 expression level (MFI) of cTfh in the different severity groups. Pairwise Wilcox test. (B) Correlation of cTfh cell number and serological responses by severity and time period. ****. Notice that significant correlations are clustered for IgM in asymptomatic and for IgM, IgA, and IgM in the different periods of severe patient's follow-up. See text for comments. $p < 0.05$*, $p < 0.01$ =**, $p < 0.001$=***, $p < 0.0001$ = ****.

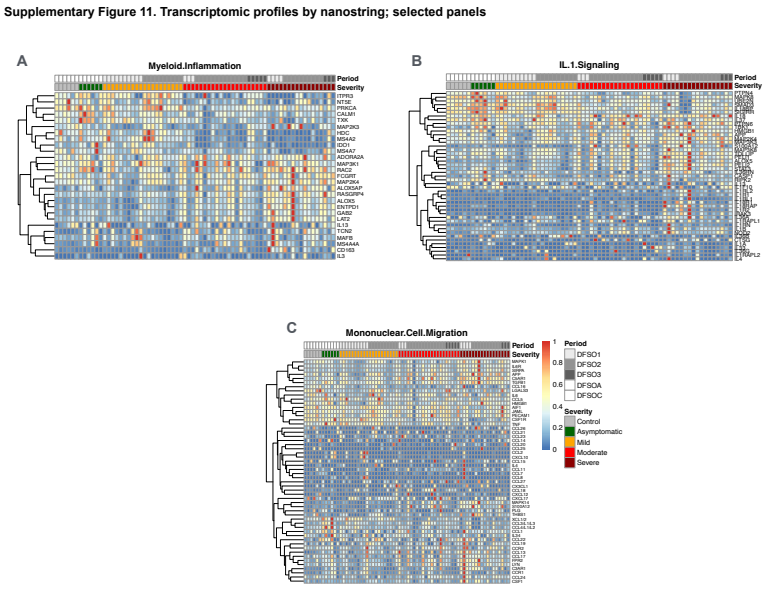

Supplemental Figure 11. **Heatmaps summarizing the transcriptomic profile of 33 COVID-19 patients stratified by severity and follow-up periods**. (A) Myeloid inflammation; (B) IL-1 signaling; and (C) Mononuclear cell Migration.

TABLES

Table 1. Patients and sample distribution across the follow periods.

			Periods															
		DFSO1 or DFSO_A or DFSO_C (0-7 days)						DFSO2 (8-20 days)						DFSO3 (21-107 days)					
		Patients	Samples					Patients	Samples					Patients	Samples				
Groups, total patients		n	Cl Chem	Cytokines	Serology	Flowcyt	Nanostr	n	Cl Chem	Cytokines	Serology	Flowcyt	Nanostr	n	Cl Chem	Cytokines	Serology	Flow cytom	Nanostr
Control	44	44	NA	24	38	44	6	NA	NA	NA	NA	NA	NA	NA	NA	NA	NA	NA	NA
Asympt	38	38	38	28	37	37	6	NA	NA	NA	NA	NA	NA	NA	NA	NA	NA	NA	NA
Mild	49	49	74	47	74	76	10	44	58	41	58	57	10	ND	ND	ND	ND	ND	ND
Moderate	64	38	45	24	45	45	3	48	74	56	73	70	13	41	47	30	46	45	5
Severe	40	19	21	13	20	19	4	36	60	45	57	58	10	19	20	16	19	19	3
Totals	235	188	178	136	214	221	29	128	192	142	188	185	33	60	67	46	65	64	8
			Time of sample																
			A					B						C					
		Patients	Samples					Patients	Samples					Patients	Samples				
		n	Cl Chem	Cytokines	Serology	Flowcyt	Nanostr	n	Cl Chem	Cytokines	Serology	Flowcyt	Nanostring	n	Cl Chem	Cytokines	Serology	Flow cyt	Nanostr
Control	44	44	NA	24	38	44	6	NA	NA	NA	NA	NA	NA	NA	NA	NA	NA	NA	NA
Asympt	38	38	38	28	37	37	6	NA	NA	NA	NA	NA	NA	NA	NA	NA	NA	NA	NA
Mild	49	44	48	30	48	49	6	44	43	29	43	43	7	41	41	29	41	41	7

Moderate	64	64	64	36	64	64	7	53	53	37	53	49	7	49	49	37	47	47	7
Severe	40	40	40	27	40	39	7	49	36	28	32	33	7	25	25	19	24	24	3
Totals	235	230	190	145	227	233	32	146	132	94	128	125	21	115	115	85	112	112	17

This table summarizes the period of patient enrolling, observation, samples and variables measured in them. In the top periods, in the bottom table the samples in the order they were taken, A, B and C. Notice that 26 moderate and 21 severe contributed their samples in period DFSO2; also that while 107 contributed three samples, 34 two and 14 one. See text section results “Features of the Barcelona COVID second-wave cohort” for details and justification.

Table 2.Summary of demographic and clinical data

	HEALTHY	ASYMPT	MILD	MODERATE	SEVERE	ALL	*p* among groups
	N (%)	N (%)	N (%)	N (%)	N (%)	N (%)	
	44 (18.7)	38 (16.2)	49 (20.9)	64 (27.2)	40 (17.0)	235	
Blood Bank	44 (100)	NA	NA	NA	NA	44 (18.7)	NA
Primary Care	0 (0)	38 (100)	47 (95.9)	5 (7.8)	1 (2.5)	91 (38.7)	NA
Hosp. Univ. Bellvitge	NA	NA	0 (0)	20 (31.3)	18 (45.0)	38 (16.2)	NA
Hosp. Univ. Germans Trias	NA	NA	1 (2.0)	22 (34.4)	9 (22.5)	32 (13.6)	NA
Hosp. Univ. Vall Hebron	NA	NA	2 (4.1)	18 (28.2)	10 (26.3)	30 (12.8)	NA
Age (median IQR)	50 [45 - 59]	41 [36- 56]	48 [35 - 62]	53 [44 - 60]	68 [55 - 73]	54 [41- 69]	2.12e-06
Age, severe vs other groups, p values (Wilcox)	3.41e-06	1.42e-04	3.90e-04	7.00e-03	NA	NA	
Sex							
Male	18 (40.9)	24 (63.2)	28 (57.1)	22 (34.4)	10 (25.0)	102 (43.4)	0.003
Female	26 (59.1)	14 (36.8)	22 (44,9)	43 (70.0)	28 (70.0)	133 (56.6)	
Toxic Habits							
Smoker	0	4 (10.5)	4 (8)	1 (1.6)	2 (5.0)	11 (5.8)	0.257
Alcohol	0	1 (2.6)	1 (2)	5 (7.8)	1 (2.5)	8 (4.3)	0.447
Comorbidities							
Psychiatric disease	0	3 (7.9)	7 (14.3)	5 (7.8)	4 (10.0)	19 (9.9)	0.674
Diabetes	0	2 (5.3)	3 (6.1)	15 (23.4)	9 (22.5)	29 (15.2)	0.010

inmunosupression	0	0 (0)	0 (0)	2 (3.1)	4 (10.0)	6 (3.1)	0.594
Solid Cancer	0	2 (5.3)	1 (2)	7 (10.9)	5 (12.5)	15 (7.9)	0.197
Active Cancer	0	0 (0)	0 (0)	0 (0)	2 (5.0)	2 (1.0)	0.052
Hypertension	0	8 (21.1)	6 (12.2)	23 (35.9)	16 (40.0)	53 (27.7)	0.006
Heart failure	0	0 (0)	0 (0)	4 (6.3)	2 (5.0)	6 (3.1)	0.151
Lung Disease	0	0 (0)	2 (4.1)	10 (15.6)	6 (15.0)	18 (9.4)	0.019
Chronic Kidney Failure	0	1 (2.6)	0 (0)	5 (7.8)	3 (7.5)	9 (4.7)	0.183
Liver Cirrhosis	0	0 (0)	0 (0)	0 (0)	1 (2.6)	1 (0.5)	0.284
Neurologic Disease	0	0 (0)	1 (2)	1 (1.6)	1 (2.5)	3 (1.6)	0.192
Charlson Score	NA	0 [0, 1.8]	0 [0, 2]	1 [0, 3]	2.5 [2, 4]	1 [0,3]	3.90e-06
Prior Medication							
Anticoagulants	NA	0 (0)	2 (4.1)	3 (4.7)	2 (5.0)	7 (3.7)	0.150
Corticosteroids	NA	0 (0)	0 (0)	3 (4.7)	3 (7.5)	6 (3.1)	0.029
Immunosupression	NA	0 (0)	0 (0)	1 (1.6)	1 (2.5)	2 (1.0)	0.029
Statins	NA	3 (7.9)	1 (2.0)	31 (48.4)	11 (27.5)	46 (24.1)	0.002
Angiot conv enzymes inhibitors	NA	4(10.5)	4 (8.2)	11 (17.2)	4(10.0)	23(12.0)	0.469
Angiotensin receptor II blockers	NA	5(13.1)	4(8.2)	3 (4.7)	10(25.0)	22(11.5)	0.013
Clinical Presentation							
Fever	NO	0 (0)	12 (24.4)	52 (81.2)	31 (77.5)	31 (16.2)	6.336e-19
Weight loss	NO	0 (0)	1 (2.04)	3 (4.68)	0 (0)	4 (2.1)	0.288
Malaise	NO	1 (100)	38 (77.5)	29 (45.3)	20 (50)	88 (46.1)	1.535e-10

Cough	NO	0 (0)	26 (53.0)	42 (65.6)	21 (52.5)	89 (46.6)	1.622e-09
Dyspnea	NO	0 (0)	0 (0)	27 (42.1)	24 (60)	51 (26.7)	1.995e-13
Expectoration	NO	0 (0)	0 (0)	2 (3.12)	1 (2.5)	3 (1.6)	0.455
Hemoptysis	NO	0 (0)	0 (0)	1 (1.56)	0 (0)	1 (0.5)	0.573
Pleuritic Chest Pain	NO	0 (0)	0 (0)	2 (3.12)	3 (7.5)	5 (2.6)	0.105
Rhinorrhea	NO	0 (0)	2 (4.08)	1 (1.56)	0 (0)	3 (1.6)	0.356
Anosmia	NO	1 (2.63)	8 (16.3)	16 (25)	6 (15)	30 (15.7)	0.032
Cacosmia	NO	0 (0)	0 (0)	1 (1.56)	2 (5)	3 (1.6)	0.219
Odinophagya	NO	0 (0)	0 (0)	7 (10.9)	2 (5)	9 (4.7)	0.020
Myalgia	NO	0 (0)	2 (4.08)	15 (23.4)	12 (30)	29 (15.2)	7.54e-05
Nausea	NO	0 (0)	1 (2.04)	9 (14.0)	6 (15)	16 (8.4)	0.012
Vomits	NO	0 (0)	0 (0)	8 (12.5)	1 (2.5)	9 (4.7)	0.004
Diarrhea	NO	0 (0)	1 (2.04)	16 (25)	12 (30)	29 (15.2)	1.557e-05
Confusion	NO	0 (0)	0 (0)	0 (0)	3 (7.5)	3 (1.6)	0.009
SpO2/FiO2, median IQR	NA	NA	466 [461 - 471]	442 [340- 461]	361 [271 - 457]	277 [165- 339]	b

NA, not applicable; *p* among groups: Kruskal-Wallis test; significant values in bold.

Table 3. Summary of laboratory data

	Control	Asymptomatic	Mild	Moderate	Severe	
Patients	44	38	49	64	40	
Clnical Chemistry	median [IQR]	median [IQR]	median [IQR]	median [IQR]	median [IQR]	p.adjust
Hb	15.00 [13.50, 16.02]	14.30 [13.62, 15.07]	14.20 [13.35, 14.95]	13.35 [12.35, 14.70]	13.20 [12.10, 14.22]	4.33E-05
WBC	6.30 [5.16, 7.77]	5.65 [4.55, 6.47]	4.50 [3.70, 5.90]	5.28 [4.10, 6.62]	7.45 [6.07, 12.66]	1.90E-07
Basophils 10e9/L	0.00 [0.00, 0.10]	0.00 [0.00, 0.00]	0.00 [0.00, 0.00]	0.00 [0.00, 0.01]	0.00 [0.00, 0.02]	6.14E-03
Basophils %	0.70 [0.50, 0.92]	0.50 [0.30, 0.70]	0.50 [0.30, 0.60]	0.30 [0.20, 0.50]	0.20 [0.10, 0.30]	1.90E-07
Eosinophils 10e9/L	0.10 [0.10, 0.20]	0.10 [0.00, 0.10]	0.10 [0.00, 0.10]	0.00 [0.00, 0.02]	0.00 [0.00, 0.01]	1.90E-07
Eosinophils %	2.05 [1.67, 3.20]	1.45 [0.83, 2.30]	1.20 [0.55, 1.85]	0.20 [0.00, 0.70]	0.00 [0.00, 0.10]	1.90E-07
Lymphos 10e9/L	1.90 [1.50, 2.42]	1.95 [1.40, 2.38]	1.60 [1.30, 1.85]	1.00 [0.86, 1.42]	0.86 [0.50, 1.20]	1.90E-07
Lymphos %	30.40 [25.65, 33.95]	35.70 [30.65, 41.08]	34.70 [28.00, 41.90]	21.30 [13.10, 26.20]	9.40 [5.25, 16.95]	1.90E-07
Monocytes 10e9/L	0.50 [0.40, 0.60]	0.50 [0.32, 0.70]	0.50 [0.40, 0.60]	0.45 [0.30, 0.60]	0.40 [0.30, 0.62]	2.79E-01
Monocytes %	7.80 [6.97, 9.05]	8.45 [7.30, 11.42]	10.20 [8.90, 13.35]	8.80 [5.55, 11.10]	5.05 [3.77, 7.82]	1.90E-07
Neutrophils 10e9/L	3.40 [2.95, 4.85]	2.75 [2.20, 3.50]	2.30 [1.80, 3.00]	3.54 [2.69, 4.72]	7.50 [4.56, 11.44]	1.90E-07
Neutrophils %	58.50 [53.48, 62.30]	50.80 [46.10, 57.95]	49.40 [44.60, 58.50]	68.85 [58.68, 80.03]	82.75 [78.05, 89.25]	1.90E-07
Platelets 10e9/L	218.50 [188.50, 255.25]	197.50 [172.50, 234.75]	197.00 [169.50, 214.50]	214.00 [164.50, 278.25]	236.00 [181.25, 327.00]	2.42E-02
C Reactive protein mg/dL (0.03–0.5 mg/dL)	ND	0.23 [0.15, 0.95]	0.39 [0.20, 1.46]	6.18 [2.41, 10.76]	11.91 [7.55, 19.55]	1.90E-07
Calprotectin	ND	1.50 [0.90, 1.96]	1.17 [0.91, 1.78]	4.80 [3.01, 9.00]	9.78 [6.14, 22.76]	1.90E-07
D-dimer (0–243 ng/mL)	ND	306.00 [251.00, 408.00]	326.00 [213.00, 517.00]	309.00 [250.00, 612.00]	417.00 [266.50, 958.25]	1.53E-01
Ferritin (25–400 ng/mL)	ND	120.50 [36.75, 283.50]	173.00 [66.50, 316.75]	415.00 [215.50, 1130.00]	738.00 [508.50, 1383.75]	1.90E-07
LDH (120-246 IU/L)	ND	171.00 [157.25, 199.25]	174.00 [158.50, 201.25]	250.00 [197.50, 331.50]	389.00 [304.50, 480.00]	1.90E-07

ALT (10-49 IU/L)	ND	20.00 [14.00, 32.00]	21.00 [15.00, 33.00]	36.00 [17.00, 61.50]	35.00 [21.75, 49.25]	1.13E-03
AST (8-34 IU/L)	ND	23.00 [18.25, 27.75]	25.00 [21.00, 32.25]	39.00 [24.50, 55.00]	39.00 [31.50, 55.00]	1.90E-07
Total Bilirrubin (0.3–1.2 mg/dL	ND	0.42 [0.31, 0.53]	0.46 [0.36, 0.62]	0.50 [0.41, 0.70]	0.53 [0.36, 0.58]	1.99E-02
Triglicerids (43 – 200 mg/dL)	ND	85.00 [69.50, 121.25]	107.00 [74.00, 133.00]	131.00 [100.00, 158.50]	134.50 [89.75, 201.75]	3.88E-04
Creatinine (0,67 - 1.17 mg/dL)	ND	0.82 [0.71, 1.02]	0.82 [0.69, 0.99]	0.81 [0.67, 0.94]	0.82 [0.71, 0.94]	9.60E-01
Urea ((17–42 mg/dL)	ND	29.40 [25.35, 35.70]	30.00 [25.80, 36.60]	33.00 [26.38, 48.45]	48.90 [39.90, 57.50]	1.90E-07
Fibrinogen ((2.39–6.1 g/L)	ND	4.63 [3.96, 5.26]	4.47 [3.91, 4.95]	6.00 [4.00, 7.00]	6.00 [5.00, 7.00]	3.54E-06
ProtrombiTime INR	ND	1.10 [1.04, 1.13]	1.10 [1.05, 1.16]	1.02 [0.98, 1.12]	1.07 [1.00, 1.13]	4.82E-02
Anti-SARS-CoV-2 Seroloyy						
Anti-SARS-CoV-2 Mpro IgM	33.26 [22.03, 47.63]	39.10 [24.23, 58.06]	33.31 [25.12, 68.87]	76.69 [28.52, 202.40]	71.48 [27.81, 246.80]	1.35E-03
Anti-SARS-CoV-2 NP IgM	19.79 [10.30, 36.46]	22.87 [12.06, 40.19]	20.17 [11.95, 52.20]	49.58 [17.15, 153.28]	44.92 [19.82, 191.47]	5.66E-04
Anti-SARS-CoV-2 S pyke IgM	11.26 [7.73, 16.63]	18.14 [11.35, 23.69]	18.27 [10.64, 50.39]	195.79 [32.00, 419.62]	166.40 [19.37, 597.09]	1.90E-07
Anti-SARS-CoV-2 RBD IgM	28.30 [18.08, 50.42]	31.68 [18.74, 51.56]	34.24 [22.47, 57.83]	27.30 [18.18, 56.10]	28.44 [13.35, 67.82]	6.45E-01
Anti-SARS-CoV-2 Mpro IgG	104.62 [79.80, 140.57]	131.61 [98.43, 213.75]	141.66 [103.37, 251.88]	2366.32 [218.92, 8961.47]	3802.74 [255.20, 17061.04]	1.90E-07
Anti-SARS-CoV-2 NP IgG	87.82 [52.94, 147.42]	108.90 [67.80, 299.94]	119.68 [65.33, 219.93]	1523.34 [213.28, 6132.72]	1675.92 [198.03, 14891.76]	1.90E-07
Anti-SARS-CoV-2 Spyke IgG	352.43 [172.59, 519.99]	482.34 [413.13, 781.45]	363.83 [287.60, 674.92]	1182.96 [479.80, 2882.23]	1409.81 [675.78, 3069.88]	1.90E-07
Anti-SARS-CoV-2 RBD IgG	151.80 [99.39, 189.06]	166.19 [141.64, 197.79]	169.66 [127.47, 230.83]	174.49 [124.02, 258.31]	206.29 [150.35, 267.33]	2.09E-02
Anti-SARS-CoV-2 Mpro IgA	63.42 [53.66, 78.82]	73.47 [52.11, 156.64]	82.32 [53.31, 147.56]	1863.08 [141.85, 7094.48]	1950.15 [170.74, 21127.41]	1.90E-07
Anti-SARS-CoV-2 NP IgA	47.75 [38.01, 66.72]	60.97 [37.51, 128.13]	65.71 [39.42, 145.72]	2233.86 [139.40, 8282.62]	1494.22 [165.56, 22643.54]	1.90E-07
Anti-SARS-CoV-2 Spyke IgA	89.72 [71.30, 133.01]	99.82 [64.31, 290.57]	219.47 [88.11, 307.64]	2401.77 [267.93, 10810.81]	3780.36 [478.96, 9936.22]	1.90E-07
Anti-SARS-CoV-2 RBD IgA	97.75 [89.98, 110.80]	101.33 [83.12, 117.93]	101.37 [91.10, 122.64]	108.62 [89.57, 152.74]	101.66 [89.19, 148.74]	2.96E-01
Cytokines and chemokines						
IFN-alpha	0.00 [0.00, 0.20]	3.52 [0.30, 25.55]	15.75 [2.17, 37.62]	15.25 [2.63, 33.75]	2.05 [0.05, 15.85]	8.68E-07

IFN-g amma	0.79 [0.64, 0.97]	2.28 [1.08, 6.73]	3.04 [1.69, 5.01]	9.61 [3.04, 24.89]	3.50 [2.10, 9.84]	1.90E-07
TNF-a lpha	12.41 [9.91, 15.28]	20.95 [16.53, 24.30]	21.94 [18.42, 27.83]	21.30 [16.84, 30.80]	21.57 [18.75, 27.06]	1.90E-07
IL 6 pg/ml	3.06 [2.33, 4.46]	3.44 [2.67, 9.15]	5.12 [3.46, 15.40]	33.85 [19.82, 56.38]	37.20 [16.10, 107.02]	1.90E-07
IL 1RA pg/ml	365.02 [269.41, 504.56]	581.58 [443.75, 922.75]	940.33 [539.00, 1548.07]	1727.37 [1281.84, 2839.75]	2190.32 [1377.82, 3004.16]	1.90E-07
IL 7 pg/ml	13.89 [10.13, 16.30]	14.15 [10.70, 18.85]	15.57 [10.61, 18.24]	21.90 [13.12, 32.41]	39.30 [25.55, 55.57]	3.58E-07
IL 12p70 pg/ml	1.16 [0.29, 2.75]	2.45 [1.68, 2.84]	2.13 [1.18, 2.93]	1.77 [1.24, 2.11]	1.60 [1.05, 2.15]	2.03E-02
IL 10 pg/ml	2.98 [1.85, 3.43]	4.46 [3.80, 8.32]	5.48 [3.63, 8.25]	12.10 [8.74, 17.90]	19.20 [11.75, 23.15]	1.90E-07
IL 13 pg/ml	6.74 [4.06, 11.20]	8.60 [3.32, 16.40]	9.33 [6.43, 15.65]	7.20 [5.62, 18.62]	8.75 [5.18, 15.72]	2.95E-01
IL 15 pg/ml	2.83 [2.09, 4.00]	3.53 [2.87, 4.98]	4.98 [3.50, 6.39]	5.35 [4.19, 7.35]	5.52 [4.61, 6.79]	3.58E-07
IL 17A pg/ml	1.17 [0.69, 2.00]	2.41 [1.71, 3.14]	2.76 [2.03, 3.90]	2.57 [2.10, 4.54]	2.58 [1.57, 3.91]	6.67E-05
IL 2 pg/ml	0.15 [0.08, 0.30]	0.30 [0.22, 0.45]	0.44 [0.32, 0.64]	0.84 [0.51, 2.04]	0.76 [0.48, 1.03]	1.90E-07
IL 4 pg/ml	0.66 [0.53, 0.78]	0.50 [0.35, 0.61]	0.58 [0.45, 0.79]	0.72 [0.47, 1.04]	0.70 [0.57, 0.86]	2.42E-02
GM-CSF pg/ml	1.62 [1.26, 2.04]	3.10 [2.29, 3.71]	2.32 [1.45, 3.04]	2.13 [1.58, 3.37]	2.98 [1.71, 4.07]	4.38E-04
TGF beta-1 pg/ml	114.50 [73.12, 151.25]	163.00 [104.00, 196.75]	169.50 [133.00, 229.25]	125.00 [47.15, 172.50]	188.00 [103.50, 289.50]	3.52E-03
CCL2 pg/ml	438.01 [338.12, 556.64]	542.00 [423.25, 675.00]	613.00 [488.55, 919.00]	653.00 [486.65, 866.25]	883.00 [489.00, 1576.64]	1.19E-03
CXCL10 pg/ml	133.50 [119.94, 165.00]	466.00 [290.50, 930.00]	878.00 [584.75, 1478.25]	1742.91 [1177.00, 2278.00]	2371.00 [1645.33, 3604.50]	1.90E-07
GRANB pg/ml	15.60 [11.30, 18.80]	33.30 [26.35, 46.75]	42.20 [26.92, 64.93]	43.35 [26.00, 65.07]	36.60 [27.55, 51.55]	1.90E-07

Supplemental Table 1. Panel Flow Cytometry Reagents

Emission Wavelength (nm)	UV	Violet	Blue	Yellow Green	Red
395	CD45RA BUV395				
420	Viability UV	CCR7 BV421			
440		CD123 SB436			
450		CD161 e450			
480		IgD BV480			
500	CD16 BUV496	CD3 BV510	CD11b BB515l		
520			IgA FITC		
550			CD14 Spark Blue 550		
570	CCR5 BUV563	IgM BV570		TIGIT PE	
580				CD4 CF568	
600		IgG BV605		CD57 PE Dazzle594	
660	CD11c BUV661	CD28 BV650			CD27 APC
680			CD45 PerCP	CD95 PE Cy5	CD56 Alexa647
690			CCR4 BB700: 5ul	CD24 PEAF610	CD19 Spark NIR 685 1.2 ul
700		CCR6 BV711	TCR γδ PerCP	CD25 PEAF700	CD127 APC-R700
730	CD62L BUV737				
750		CXCR5 BV750			
780		PD-1 BV785		CXCR3 PE Cy7:2.5ul	HLA DR APC Fire
800	CD8 BUV805: 1.2 ul				CD38 APC-CF820

Supplemental table 2. B cell subset statistics

Period	Subset B cell	Compared groups		p.adj	p.adj.signif
DFSO1	B cell n	Mild	Moderate	1.16E-07	****
DFSO1	B cell n	Mild	Severe	5.61E-21	****
DFSO1	B cell n	Moderate	Severe	1.31E-08	****
DFSO2	B cell n	Mild	Moderate	1.58E-33	****
DFSO2	B cell n	Mild	Severe	6.99E-08	****
DFSO2	B cell n	Moderate	Severe	1.00E-03	**
DFSO3	B cell n	Moderate	Severe	4.00E-03	**
DFSO1	B transitional	Mild	Moderate	9.00E-03	**
DFSO1	B transitional	Mild	Severe	1.08E-79	****
DFSO1	B transitional	Moderate	Severe	1.07E-51	****
DFSO2	B transitional	Mild	Moderate	2.51E-56	****
DFSO2	B transitional	Mild	Severe	5.70E-57	****
DFSO2	B transitional	Moderate	Severe	2.55E-01	ns
DFSO3	B transitional	Moderate	Severe	2.38E-65	****
DFSO1	B naive	Mild	Moderate	1.00E+00	ns
DFSO1	B naive	Mild	Severe	2.00E-17	****
DFSO1	B naive	Moderate	Severe	6.72E-15	****
DFSO2	B naive	Mild	Moderate	2.28E-41	****
DFSO2	B naive	Mild	Severe	1.14E-05	****
DFSO2	B naive	Moderate	Severe	9.33E-14	****
DFSO3	B naive	Moderate	Severe	1.20E-01	ns
DFSO1	B unswitched mem	Mild	Moderate	1.37E-13	****
DFSO1	B unswitched mem	Mild	Severe	4.62E-11	****
DFSO1	B unswitched mem	Moderate	Severe	1.00E-02	**
DFSO2	B unswitched mem	Mild	Moderate	8.49E-21	****
DFSO2	B unswitched mem	Mild	Severe	1.70E-02	*
DFSO2	B unswitched mem	Moderate	Severe	2.30E-05	****
DFSO3	B unswitched mem	Moderate	Severe	1.63E-01	ns
DFSO1	B IgM only mem	Mild	Moderate	3.15E-70	****
DFSO1	B IgM only mem	Mild	Severe	6.78E-25	****
DFSO1	B IgM only mem	Moderate	Severe	6.00E-03	**
DFSO2	B IgM only mem	Mild	Moderate	9.99E-84	****
DFSO2	B IgM only mem	Mild	Severe	1.78E-63	****
DFSO2	B IgM only mem	Moderate	Severe	1.00E+00	ns

DFSO3	B IgM only mem	Moderate	Severe	2.40E-01	ns
DFSO1	B mem IgA	Mild	Moderate	2.02E-106	****
DFSO1	B mem IgA	Mild	Severe	5.88E-39	****
DFSO1	B mem IgA	Moderate	Severe	2.65E-01	ns
DFSO2	B mem IgA	Mild	Moderate	8.58E-72	****
DFSO2	B mem IgA	Mild	Severe	5.88E-79	****
DFSO2	B mem IgA	Moderate	Severe	7.89E-01	ns
DFSO3	B mem IgA	Moderate	Severe	3.96E-05	****
DFSO1	B mem IgG	Mild	Moderate	1.85E-72	****
DFSO1	B mem IgG	Mild	Severe	6.09E-60	****
DFSO1	B mem IgG	Moderate	Severe	1.10E-07	****
DFSO2	B mem IgG	Mild	Moderate	7.05E-119	****
DFSO2	B mem IgG	Mild	Severe	7.50E-123	****
DFSO2	B mem IgG	Moderate	Severe	2.00E-03	**
DFSO3	B mem IgG	Moderate	Severe	1.07E-01	ns
DFSO1	B switched resting	Mild	Moderate	3.36E-79	****
DFSO1	B switched resting	Mild	Severe	1.48E-63	****
DFSO1	B switched resting	Moderate	Severe	1.75E-05	****
DFSO2	B switched resting	Mild	Moderate	2.43E-85	****
DFSO2	B switched resting	Mild	Severe	7.14E-69	****
DFSO2	B switched resting	Moderate	Severe	1.00E+00	ns
DFSO3	B switched resting	Moderate	Severe	3.69E-05	****
DFSO1	B switched act	Mild	Moderate	4.83E-114	****
DFSO1	B switched act	Mild	Severe	1.04E-45	****
DFSO1	B switched act	Moderate	Severe	4.20E-01	ns
DFSO2	B switched act	Mild	Moderate	8.16E-73	****
DFSO2	B switched act	Mild	Severe	3.84E-84	****
DFSO2	B switched act	Moderate	Severe	7.10E-02	ns
DFSO3	B switched act	Moderate	Severe	6.04E-01	ns
DFSO1	B DN1	Mild	Moderate	4.92E-15	****
DFSO1	B DN1	Mild	Severe	2.44E-28	****
DFSO1	B DN1	Moderate	Severe	1.93E-08	****
DFSO2	B DN1	Mild	Moderate	9.03E-39	****
DFSO2	B DN1	Mild	Severe	3.06E-46	****
DFSO2	B DN1	Moderate	Severe	4.10E-02	*
DFSO3	B DN1	Moderate	Severe	9.40E-05	****
DFSO1	B DN2	Mild	Moderate	6.78E-17	****
DFSO1	B DN2	Mild	Severe	7.77E-01	ns
DFSO1	B DN2	Moderate	Severe	8.13E-06	****
DFSO2	B DN2	Mild	Moderate	3.33E-17	****
DFSO2	B DN2	Mild	Severe	6.00E-02	ns
DFSO2	B DN2	Moderate	Severe	3.93E-21	****

DFSO3	B DN2	Moderate	Severe	4.05E-19	****
DFSO1	B unclassified	Mild	Moderate	1.81E-17	****
DFSO1	B unclassified	Mild	Severe	3.99E-13	****
DFSO1	B unclassified	Moderate	Severe	1.52E-01	ns
DFSO2	B unclassified	Mild	Moderate	4.74E-38	****
DFSO2	B unclassified	Mild	Severe	3.75E-06	****
DFSO2	B unclassified	Moderate	Severe	1.36E-10	****
DFSO3	B unclassified	Moderate	Severe	1.59E-04	***